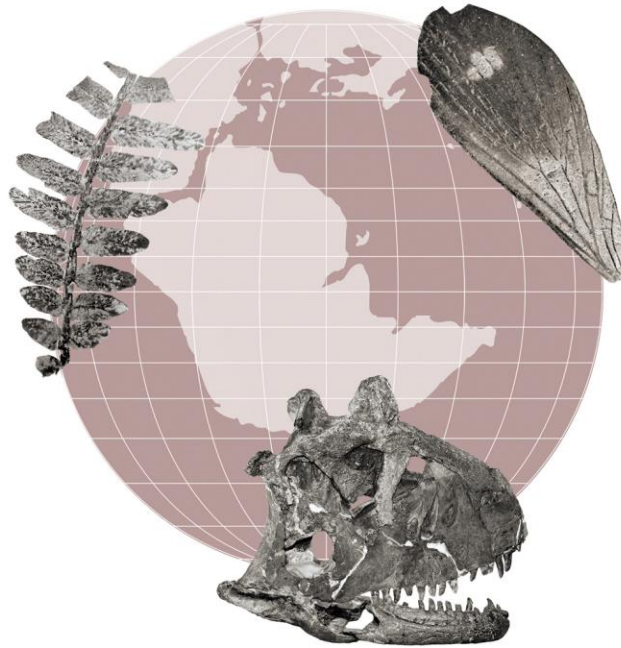




# AMEGHINIANA

A GONDWANAN PALEONTOLOGICAL JOURNAL



This file is an uncorrected accepted manuscript (i.e., postprint). Please be aware that this version will change during the production process. This postprint will be removed once the paper is officially published. All legal disclaimers that apply to the journal pertain.

**Submitted:** 10 September 2025 - **Accepted:** 16 March 2026 - **Posted online:** 30 March 2026

To link and cite this article:

**doi:** [10.5710/AMGH.16.03.2026.3670](https://doi.org/10.5710/AMGH.16.03.2026.3670)

PLEASE SCROLL DOWN FOR ARTICLE

1 **A reappraisal of *Palmoxylon* (Arecaceae) species from the uppermost Cretaceous Allen**  
2 **Formation, Río Negro Province, Argentinian Patagonia**

3

4 Ezequiel I. Vera<sup>1</sup>

5 <sup>1</sup>División Paleobotánica, Museo Argentino de Ciencias Naturales “Bernardino Rivadavia”  
6 (CONICET), Av. Ángel Gallardo 470, Ciudad Autónoma de Buenos Aires, C1405DJR,  
7 Argentina

8

9 46 pages (text + references); 7 figures; 1 table

10

11 Running Header: Vera: Cretaceous *Palmoxylon* species from Allen Formation

12

13 Short Description: Three species of *Palmoxylon* described from the uppermost Cretaceous  
14 Allen Formation are restudied and new information is provided.

15

16 Corresponding author: Ezequiel Ignacio Vera, Museo Argentino de Ciencias Naturales  
17 “Bernardino Rivadavia” (CONICET), Av. Ángel Gallardo 470, Ciudad Autónoma de Buenos  
18 Aires, C1405DJR, Argentina, [ezequiel.vera@gmail.com](mailto:ezequiel.vera@gmail.com) / [evera@macn.gov.ar](mailto:evera@macn.gov.ar)

19

20 **Abstract**

21 Three species of *Palmoxylon* Schenk, namely *P. santarosense*, *P. rionegrense* and *P.*  
22 *valchetense*, were described by Ancibor in 1995 for the uppermost Cretaceous (Campanian to  
23 Maastrichtian) Allen Formation at the Bajo de Santa Rosa locality, in northern Patagonia,  
24 Argentina. A revision of the original specimens, as well as previously unpublished remains, is  
25 carried out in light of modern descriptive procedures for palm stems. The diagnoses of the  
26 three species are emended to include new characters, as well as modifications on states of  
27 characters originally described. Epitypes for *P. santarosense* and *P. valchetense* are defined,  
28 to include more complete stems that allow a better characterization of these taxa. *P.*  
29 *rionegrense* is found referable to the subfamily Coryphoideae, with probable affinities to the  
30 tribe Caryoteae, while *P. valchetense* is referred to the tribe Trachycarpeae. *P. santarosense*  
31 is not referred to any subfamilial category due to inconclusive affinities. Affinities of these  
32 taxa provide wide climatic inferences, as they support tropical and non-tropical climates. The  
33 presence of Trachycarpeae in the latest Cretaceous of Patagonia challenges postulated  
34 divergence time estimations and biogeographic routes for this tribe.

35 **Keywords.** Trachycarpeae. Coryphoideae. Campanian. Maastrichtian. Palms. *Stipitichnus*.

36

37 **Resumen**

38 Reevaluación de especies de *Palmoxylon* (Arecaceae) del Cretácico Superior de la Formación  
39 Allen, provincia de Río Negro, Patagonia Argentina. Tres especies de *Palmoxylon* Schenk, *P.*  
40 *santarosense*, *P. rionegrense* y *P. valchetense*, fueron descriptas por Ancibor en 1995 para la  
41 Formación Allen del Cretácico Superior (Campaniano–Maastrichtiano) en la localidad de  
42 Bajo de Santa Rosa, en el norte de la Patagonia, Argentina. Se lleva a cabo una revisión de

43 los ejemplares originales, así como de restos inéditos, teniendo en cuenta procedimientos  
44 descriptivos modernos para estípites de palmeras. Se enmiendan las diagnosis de las tres  
45 especies para incluir nuevos caracteres, así como modificaciones en los estados de los  
46 caracteres originalmente descritos. Se definen epítipos para *P. santarosense* y *P.*  
47 *valchetense*, con el fin de incluir materiales más completos que permitan una mejor  
48 caracterización de estos taxones. *P. rionegrense* es interpretada como referible a la subfamilia  
49 Coryphoideae, con probables afinidades con la tribu Caryoteae, mientras que *P. valchetense*  
50 se asigna a la tribu Trachycarpeae. *P. santarosense* no es referida a ninguna categoría  
51 subfamiliar debido a que presenta afinidades no concluyentes. Las afinidades de estos  
52 taxones producen amplias inferencias climáticas, ya que son registradas tanto en climas  
53 tropicales como no tropicales. La presencia de Trachycarpeae en el Cretácico Tardío de  
54 Patagonia contrasta con las estimaciones postuladas de tiempos de divergencia y de rutas  
55 biogeográficas para esta tribu.

56 **Palabras clave.** Trachycarpeae. Coryphoideae. Campaniano. Maastrichtiano. Palmeras.  
57 *Stipitichnus*.

## 58 **Introduction**

59 The Allen Formation is an uppermost Cretaceous unit cropping out in Northern Argentinian  
60 Patagonia, and is well known by its paleontological content, first preliminarily reported by  
61 Andreis *et al.* (1991) who, since its discovery, pointed out its importance. Numerous  
62 vertebrate remains come from its strata, and include fishes (*e.g.*, Agnolín, 2010b; Bogan *et*  
63 *al.*, 2011), frogs (*e.g.*, Agnolín, 2012; Gómez, 2016; Suazo Lara & Gómez, 2022), turtles  
64 (*e.g.*, Agnolín *et al.*, 2025; Sterli *et al.*, 2013), lizards (*e.g.*, Garberoglio *et al.*, 2025),  
65 plesiosaurs (O’Gorman, 2011), mammals (*e.g.*, Rougier *et al.*, 2009; Connelly *et al.*, 2024),  
66 pterosaurs (Novas *et al.*, 2012), birds (*e.g.*, Clarke & Chiappe, 2001; Agnolín, 2010a), and  
67 several non-avian dinosaurs (*e.g.*, Salgado & Coria, 1993; Novas *et al.*, 2009; García &  
68 Salgado, 2011; Agnolín *et al.*, 2012; Cruzado Caballero & Powell, 2017; Aranciaga Rolando  
69 *et al.*, 2021; Rigueti *et al.*, 2022; Rozadilla *et al.*, 2021; Álvarez Nogueira *et al.*, 2025).  
70 Contrasting, the fossil plant record of this unit is scarce, and consist of cycad stems (Artabe *et*  
71 *al.*, 2004, 2005; Martínez *et al.*, 2012), conifer woods (Del Fueyo, 1998; Passalia *et al.*,  
72 2023), palm stems and fruits (Ancibor, 1995), and few palynological assemblages (Vallati,  
73 2010; Pérez Pincheira & Garrido, 2024). Several insect and fungal traces have also been  
74 reported from the unit, most of them associated with plant stems and fruits (Genise, 1995;  
75 Genise *et al.*, 2012).

76         Understanding ecosystem dynamics during the latest Cretaceous is critical for  
77 evaluating the effects of the end-Cretaceous extinction and reconstructing ecosystem  
78 characteristics prior to this event. In this context, making precise comparisons between fossil-  
79 bearing units across different time intervals or sedimentary basins with strata close to the K-  
80 Pg requires equally precise and comparable taxonomic data. The three *Palmoxyton* species  
81 described by Ancibor (1995) are significant because they were the first Mesozoic species for

82 the genus reported from South America. Unfortunately, the descriptions and species  
83 diagnoses provided by the author were rather brief and many key characters were missing.  
84 Furthermore, some images are not clear enough to show the non-described characters. Since  
85 these descriptions have been widely used for comparative purposes, a revision of these  
86 *Palmoxylon* species was needed, focused on describing and properly illustrating the  
87 characters currently used in anatomical descriptions of Arecaceae stems (*e.g.*, Thomas & De  
88 Franceschi, 2013), while also incorporating previously undescribed specimens. Such revision  
89 allows not only improving the knowledge of fossil palm species that were present prior to the  
90 end-Cretaceous mass extinction in Patagonia, but also adjusting their descriptions, which will  
91 provide information regarding their botanical affinities within the Arecaceae and,  
92 consequently, will allow their use as paleoclimatic proxies.

93 **Anatomical abbreviations.** TS, transverse section; LS, longitudinal section; CT, cortex; SZ,  
94 subcortical zone; CZ, central zone; TZ, transition zone; fvb, fibrovascular bundle; dcap,  
95 fibrous part adjacent to the phloem; vcap, fibrous part adjacent to the xylem; f/v, average  
96 ratio between the fibrous part and the vascular part of the fvbs; FCI, fibrous covering index,  
97 the ratio between the surface area of the fibrous part of all the fvbs in an examined transverse  
98 section and the whole surface area of the examined transverse section.

99

## 100 **Materials and Methods**

101 Studied specimens were originally collected during a field trip in the 90's by Drs. Sergio  
102 Archangelsky, Renato Andreis, Gerardo Cladera, Jorge Genise, Georgina del Fueyo and Luis  
103 Lezama, and offered to Dr. Elena Ancibor for study. They were obtained at Estancia "El  
104 Palenque" (39°58'33.88"S, 66°45'2.91"W; Genise pers. comm.), 10 km west of Santa Rosa  
105 locality and 60 km northwestern to Nahuel Niyen, Río Negro Province, Argentina, at a site

106 named “Cañadón de Marcelo” (located at the north of the Estancia “El Palenque”).  
107 Information accompanying the fossil palms mention the reference “Bosque 2, Río Negro,  
108 Bajo Santa Rosa”. Salgado *et al.* (2007) presented stratigraphic logs for the Salitral de Santa  
109 Rosa (=Bajo Santa Rosa) locality, highlighting the presence of fossil trunks in a fossiliferous  
110 level approximately at the half of the unit (Salgado *et al.*, 2007; fig. 2). The fossils palms  
111 collected at this locality, including the ones here studied, can be referred to this fossiliferous  
112 level (Salgado, pers. comm.). For a geological characterization of the unit at the Bajo Santa  
113 Rosa, see Salgado *et al.* (2007).

114 All specimens studied by Ancibor (1995) are housed in the Colección Nacional de  
115 Paleobotánica of the Museo Argentino de Ciencias Naturales “Bernardino Rivadavia” under  
116 BA Pb (hand specimens) and BA Pb Pm (microscope slides) numbers. Corresponding  
117 numbers of these specimens are 862, 879, 880, 884 (BA Pb Pm 263, 264, 265), 887 (BA Pb  
118 Pm 266, 267, 268), 888, 889, 890 (BA Pb Pm 257, 258, 259, 260, 261, 262) and 944. The  
119 specimen mentioned by Ancibor (1995) as BA Pb 878, as well as microscope slides obtained  
120 from specimens different than the holotypes of the three species, are currently not present in  
121 the Colección Nacional de Paleobotánica of the MACN, as informed by the Curatorial  
122 Technician of the collection (Lezama, pers. comm.), and its current location is unknown.

123 Specimens BA Pb 881 and 967, not included in the original publication by Ancibor (1995),  
124 were revised in this contribution. In addition, the specimen MACN-Icn 123, housed in the  
125 Colección Nacional de Icnología of the Museo Argentino de Ciencias Naturales “Bernardino  
126 Rivadavia” (originally housed in the Colección Nacional de Entomología of the same  
127 institution, under number 53816) was revised, as it was published as an Arecaceae stem  
128 containing the holotype of the ichnospecies *Stipitichnus koppae* Genise 1995, traces  
129 interpreted as insect borings, from the Bajo de Santa Rosa locality (Genise, 1995).

130 The fossil palm remains were originally thin-sectioned in TS and LS. Study was carried out  
131 using light Microscopy (Olympus BX-51 and Nikon SMZ-2 t Microscopes with attached  
132 cameras) on thin sections and polished and non-polished stems. Preservation quality varies  
133 between specimens, and some features are not observed. In particular, available longitudinal  
134 sections were scarcely informative due to preservation quality, and only few characters are  
135 described from them. Measurements were made using ImageJ free software. At least 25  
136 measurements were made for each character, when possible. For descriptions based on  
137 several specimens, weighted mean is presented (along with total size range).

138 Descriptive terminology used here follows the proposal of Thomas and De Franceschi  
139 (2013). For clarity's sake, some abbreviations used in the text are included below. The  
140 classification scheme follows Dransfield *et al.* (2008). For comparative purposes, the  
141 specimens referred to *Palmoxylon* specimens described by Vera *et al.* (2024) from the  
142 Campanian to lowermost Maastrichtian Puntudo Chico Formation were revised.  
143 Additionally, the Palm-ID online database (Thomas, 2011a), Thomas (2011b) doctoral thesis,  
144 and Thomas and De Franceschi (2013) were primarily consulted for comparisons with extant  
145 taxa.

146

## 147 **Systematic Paleontology**

148 Order Arecales Bromhead 1840

149 Family Arecaceae C.H. Berchtold et J. Presl, nom. cons. 1820

150 Fossil genus *Palmoxylon* Schenk 1882

151 **Type species.** *Palmoxylon angulare* (Cotta) Schenk 1882, from the Cenozoic of India.  
152 Originally published as *Perfossus angularis* Cotta.  
153  
154 *Palmoxylon santarosense* Ancibor 1995 *emend.* Vera  
155 Figures 1–3  
156 1995. *Palmoxylon santarosense* Ancibor. *Ameghiniana* 32(3): 298, Plate II  
157  
158 **Holotype.** BA Pb 887 (BA Pb Pm 266, 267, 268)  
159 **Epitype here designed.** BA Pb 862  
160 **Additional specimens.** BA Pb 879, 880, 944, MACN-Icn 123  
161 **Geographic occurrence.** Estancia El Palenque, 10 km west of Santa Rosa locality and 60 km  
162 northwestern to Nahuel Niyeu, Río Negro Province, Argentina, at a site named “Cañadón de  
163 Marcelo” (Bosque 2).  
164 **Stratigraphic occurrence.** Allen Formation; Upper Cretaceous (upper Campanian to  
165 Maastrichtian).  
166 **Original diagnosis (translated from Ancibor (1995), originally in Spanish).** Radially  
167 extended fibrovascular bundles; 1–2 metaxylem vessels per fibrovascular bundle; small-  
168 lumen fibers forming a bulky cap on the phloem side; phloem generally in a single, highly  
169 lobulated strand; interfascicular parenchyma with thin walls and no particular arrangement;  
170 siliceous corpuscles are spherical and slightly spiculated.

171 **Emended diagnosis.** Stem atactostelic, divided in CZ, SZ and developed CT. Ground tissue  
172 composed of isodiametric parenchymatous cells without lacunae in the outer region of the CZ  
173 and SZ, and isodiametric and elongate cells in the center of the CZ, with interspersed fibrous  
174 bundles in the outer region of the CZ and in the SZ and the CT; growth pattern *Corypha*-type;  
175 density of fvbs in the center of the stem c. 113–132 per cm<sup>2</sup> and in the subcortical zone is c.  
176 505–529 per cm<sup>2</sup>; f/v ratio c. 1–1.6 in the most internal zone of the CZ and c. 4.3–7.7 in the  
177 most external region of the SZ; CT developed; fvbs with dcap Lunaria to Vaginata in the  
178 most internal fibrovascular bundles, Reniforma towards the outer region of the CZ, and  
179 Reniforma to Sagittata in the SZ, with rounded median sinus; vcap present, tabular  
180 parenchyma present, radiating parenchyma absent; phloem undivided; xylem part presenting  
181 wide metaxylem vessels, mostly 2 in the CZ and 1 in the SZ, excluded in the outer region of  
182 the CZ and in the SZ; end walls of metaxylem elements with long scalariform plates; slope of  
183 end walls extremely to very oblique; presence of globular echinate phytoliths in axial series  
184 of stigmata at the margins of the fibrous bundles and fibrous part of the fvbs.

185 **Description.** The description is partially based on the holotype specimen BA Pb 887,  
186 consisting of a fragment of stem c. 9.2 cm in maximum width and 5.7 cm tall (Fig. 1A). The  
187 fossil preserves a portion of the internal zone of the stem. Internally, it consists of  
188 parenchymatous ground tissue and scattered fvbs, arranged in an atactostele. Other  
189 specimens, referred by Ancibor (1995) to this species, as well as others not included in the  
190 original work, were studied and complementary information was derived from them. In  
191 particular, specimen BA Pb 862 preserves a more complete transverse section of the stem,  
192 showing the distribution of fvbs in the central and outer zones (Fig. 1B). Specimens BA Pb  
193 879 and 880 preserve adventitious roots, but preservation is not good.

194 **Stem.** In the holotype (BA Pb 887), the density of fvbs in the most internal zone of the CZ is  
195 216–245 per cm<sup>2</sup>. Density in the most external preserved region of the CZ is 291 per cm<sup>2</sup>  
196 (Fig. 1A). Measured f/v ratio for fvbs is 2.1–4.3 in the most internal zone and 5–8.5 in the  
197 most external zone preserved. In the specimen BA Pb 862 (Fig. 1B, C) a more extensive  
198 portion of the stem is present, preserving from the most internal region of the CZ towards the  
199 SZ, even showing a small portion of the CT. This specimen exhibits changing density and  
200 morphology of fvbs from the most internal zone towards the periphery (Fig. 1C), and thus the  
201 ratios calculated above are measured for this specimen as well. The density of fvbs in the  
202 center of CZ is 113–132 per cm<sup>2</sup>. Density in the most external region of the SZ is 505–529  
203 per cm<sup>2</sup>. (Fig. 1C). Ratio of density of fvbs in the most external zone (SZ) vs density in the  
204 most internal zone (CZ) c. 4.26. Measured f/v for fvbs is 1–1.6 in the most internal zone  
205 ( $f/v_{in}$ ) and 4.3–7.7 in the most external region of the SZ ( $f/v_{out}$ ). Ratio between  $f/v_{out} / f/v_{in}$  c.  
206 4.6. Fibrous covering index is 0.07–0.12 in the most internal region of the CZ ( $FCI_{in}$ ) and  
207 0.41–0.47 in the subcortical zone ( $FCI_{out}$ ). Ratio between  $FCI_{out}$  and  $FCI_{in}$  is 4.63. All these  
208 parameters, along with the absence of tangential differentiation of the fibrous part of the fvbs,  
209 are in agreement with a *Corypha*-type growth pattern (von Mohl, 1823–1850; Thomas & De  
210 Franceschi, 2013).

211 **Fibrovascular bundles.** Fibrovascular bundles vary in morphology across the stem, from the  
212 center of the CZ to the SZ (Fig. 1C–E, Fig. 2A–H). Proportionally, most of the fvbs in the  
213 stem show the morphology of the outer CZ, which are observed in the holotype, and are  
214 described first. These fvbs are 530–751 ( $650 \pm 58$ )  $\mu\text{m}$  tall and 318–567 ( $462 \pm 67$ )  $\mu\text{m}$  wide.  
215 Tabular parenchyma present, consisting of 2 layers of elongate cells. Radiating parenchyma  
216 absent. Fibrous part Reniforma in shape (Stenzel, 1904), with absent auricular sinuses (Fig.  
217 2A–D). Fibrous part centrifugal differentiation not observed. Median sinus rounded (Fig. 2D–  
218 E). Dorsal cap 291–480 ( $376 \pm 48$ )  $\mu\text{m}$  high, composed of a dense mass of fibers (Fig. 2D–E).

219 Fibers 12.5–25.6 (19.7±4) μm in diameter, with thick walls. Ventral cap present (Fig.2B–E),  
220 crescentiform, composed of cells 10.4–22.4 (14±3.2) μm in diameter, thick walled,  
221 sometimes connecting with dcap. The xylem part of the fibrovascular bundles consist of  
222 typically 2 (rarely 1) excluded, adjacent (touching) wide metaxylem elements (Fig. 2A–E)  
223 65.6–175.6 (132.6±17.7) μm in diameter, with end walls exhibiting long scalariform plates  
224 (Fig. 2O), with many closely spaced bars; metaxylem end wall slope extremely oblique to  
225 very oblique (Fig. 2O) (measured on 3 perforation plates, with values of 12, 8 and 5);  
226 paravascular parenchyma poorly developed. Small vessels (protoxylem?) observed in some  
227 fibrovascular bundles, located adjacent to the contact between wide metaxylem elements  
228 (Fig. 2E). Phloem region is located in the zone between the xylem and the dcap. Its shape is  
229 triangular with rounded apices to reniform (Fig. 2C–E), often appearing with irregular forms,  
230 and sometimes showing a small interruption as a result of a projection of the dcap (Fig. 2C).  
231 Sieve cells 11.4–24.2 (17.1±4.3) μm in diameter; smaller elements of the phloem (companion  
232 cells?) 5.1–7.8 (6.8±1) μm in diameter (Fig. 2E). Metaphloem sieve plate not observed.

233 Fibrovascular bundles in the SZ are 639–733 (677±31) μm tall and 156–265 (223±43) μm  
234 wide (Fig. 2F–G). Anatomically, they share the features of the ones present in the CZ, but  
235 differ in having typically a single (rarely two) wide metaxylem element 74.7–108.3  
236 (92.1±11.3) μm in diameter (Fig. 2F–G). Most distal fvbs exhibit slightly elongate fibrous  
237 portions of the fvbs (Fig. 2F), with a ratio between the height of the dcap - height of the  
238 vascular portion of the fvb) / width of the fvb of ranging from 1.1–2.1, thus not considered as  
239 having radial elongation of the fibrous part (in the SZ), as proposed for Descriptor 8 in  
240 Thomas and De Franceschi (2013). Fibrovascular bundles with most elongate portions  
241 showing a morphology of the dcap close to Sagittata in shape (Fig. 2F).

242 Fibrovascular bundles in the most internal part of the CZ are smaller than the previously  
243 described from the SZ and the outer region of the CZ, 374–694 (598±102) µm tall and 379–  
244 539 (452±61) µm wide (Fig. 1D–E). The dcap is Lunaria to Vaginata in shape, and the  
245 vascular portion exhibits 2 large metaxylem vessels, 196–236 (219±13) µm wide (Fig. 1D–  
246 E).

247 **Ground tissue.** In the Holotype BA Pb 887, ground tissue is essentially parenchymatous,  
248 mostly composed of isodiametric, spheroidal to slightly elongate, thin-walled cells, 17.4–55.1  
249 (30.7±10.7) µm in diameter, constituting a compact tissue without lacunae or intercellular  
250 spaces (Fig. 2J). The more complete specimen BA Pb 862, ground tissue exhibits the same  
251 features in the outer region of the CZ and in the SC, but the inner region of the CZ also shows  
252 elongate cells 76.4–139.6 (114.4±26.2) µm in long and 23.7–39.5 (34.6±6.5) µm wide (Fig.  
253 2I). It is unclear if sparse lacunae are present between elongate cells.

254 Interspersed in the parenchymatous tissue of the most external region of the CZ, in the SZ  
255 and in the CT, fibrous bundles are present. These bundles are circular to oval in cross section.  
256 48–73.3 (59.5±8.5) µm in diameter (Fig. 2F, H, K). In addition, the cortical zone exhibits  
257 larger fibrous bundles, 112–171 (140±22) µm in diameter (Fig. 2H, K).

258 **Phytoliths.** In the longitudinal section of the holotype, globular granulate phytoliths 8–15.2  
259 (12.4±3) µm in diameter are present in stigmata in the marginal region of the fibrous part of  
260 the fvbs (Fig. 2P).

261 **Leaf traces.** Several bundles with fibrous and vascular components differ in their structure  
262 and size from the typical fvbs, and are interpreted as leaf traces. They are 568–845 (732±92)  
263 µm tall and 341–627 (496±102) µm wide (Fig. 2L–M). They contain two xylem regions. The  
264 central one consists of 2 (rarely 3) separate wide metaxylem elements 69.5–122.5 (98±17.1)  
265 µm wide; while the ventral group is composed of several smaller elements, 19.5–51

266 (31.2±9.8) µm wide (Fig. 2M). Phloem region in these structures appears typically as  
267 composed of 2– 3 interconnected lobes. Towards the SZ/CT, leaf traces often show a higher  
268 number of smaller metaxylem elements in the central group.

269 **Vascular bridges.** Several small bundles are present in the ground tissue, often adjacent (and  
270 opposite oriented) to leaf traces. They are 202–380 (297±73) µm tall and 167–346 (288±74)  
271 µm wide. They show an anatomy comparable to the one observed in the fvbs of the CZ, but  
272 have a dcap similar or smaller in size than the vascular part (Fig. 2L, N).

273 **Cortical zone.** A small portion of this region is preserved in BA Pb 862. The maximum  
274 measured thickness is approximately 1 mm, but the externalmost limit is unpreserved. It  
275 exhibits parenchymatic ground tissue with interspersed small and large fibrous bundles, and  
276 scarce vascular bundles (Fig. 2H, K), but is unclear if it corresponds to fvbs or leaf traces due  
277 to preservation quality,

278 **Remarks.** The holotype specimen (BA Pb 887) selected by Ancibor (1995) preserves a  
279 portion of the most external region of the CZ of the stem. Among the rest of the specimens  
280 available of this species, BA Pb 862 preserves a complete transverse section of CZ and SZ, as  
281 well as a small portion of the CT. Given its informative value, which was used for providing  
282 an emended diagnosis for the species, it is here designated as an epitype of *Palmoxylon*  
283 *santarosense* (ICN Art. 9.9).

284 Ancibor (1995) listed specimen BA Pb 826 among the referred to this species (Ancibor,  
285 1995; p. 298), but it does not correspond with a *Palmoxylon* stem (Lezama & Del Fueyo,  
286 pers. comm.). It is clear that it was an involuntary error, as the author lists in the same work  
287 the specimen BA Pb 862 (and not 826) as belonging to the “Grupo I” (Ancibor, 1995; p.  
288 292), which is equivalent to *Palmoxylon santarosense*.

289 The specimen MACN-Icn 123, containing the holotype of the ichnospecies *Stipitichnus*  
290 *koppae* Genise 1995 (traces interpreted as insect borings) has an anatomy comparable with  
291 *Palmoxylon santarosense* (Fig. 3), and comparisons with available specimens of this latter  
292 taxon allowed the recognition of BA Pb 944 as a slide of the stem containing the ichnofossils  
293 MACN-Icn 123.

294 **Comparisons with fossil forms from South America.** Several species of *Palmoxylon* have  
295 been recorded in South America (Table 1), but no one shares with *Palmoxylon santarosense*  
296 the presence of fvbs with typically 2 wide metaxylem elements in the CZ and 1 in the SZ  
297 (Fig. 2A–C, F, G). Fragmentary taxa that are completely unknown that have a single (or 1–2)  
298 wide metaxylem vessels per fvb include *Palmoxylon* sp. 3 in Vera *et al.* (2024), and  
299 *Palmoxylon* sp. 4 in Vera *et al.* (2024), and *Palmoxylon chilense* (Torres & Godoy, 1982).  
300 *Palmoxylon* sp. 3 in Vera *et al.* (2024) and *Palmoxylon* sp. 4 in Vera *et al.* (2024) exhibit fvbs  
301 from the SZ having Reniforma shape of the dcap (Table 1), different from the typical  
302 Sagittata form observed in *P. santarosense* (Fig. 2F, G). On the other hand, *P. chilense* has  
303 fvbs with a single wide metaxylem element in the CZ and SZ (Table 1), while in *P.*  
304 *santarosense* the fvbs of the CZ typically have 2 wide metaxylem elements, and 1 only in the  
305 outer region of the SZ (Fig. 2A–C, F, G). In addition, *P. chilense* has radiating parenchyma  
306 (Table 1), absent in the specimens here studied.

307 **Comparisons with extant taxa and affinities.** Extant Arecaceae exhibiting fvbs with two  
308 wide metaxylem vessels in the CZ and one in the SZ are present in the genera *Caryota* L. and  
309 *Arenga* Labill. of the Coryphoideae tribe Caryoteae, *Eugeissona* Griff., *Mauritia* L. and  
310 *Raphia* P. Beauv. of the Calamoideae, and in the Arecoideae (Thomas, 2011a, b; Thomas &  
311 De Franceschi, 2013). Thomas and Boura (2015) suggested that the fvbs having a single wide  
312 metaxylem element (or having two in the CZ but changing to one in the SZ) were probably

313 an apomorphic condition, whereas two vessels were plesiomorphic.

314 Thomas and De Franceschi (2013) state that *Caryota* and *Arenga* of the Caryoteae have  
315 typically *Mauritia*-type of stem organization, with a tendency towards *Corypha*-type (the  
316 latter state present in *P. santarosense*). Nevertheless, this tribe exhibits radial differentiation  
317 of the fibrous part, and trapeziform and combined phytoliths (Thomas & De Franceschi,  
318 2013), both absent in *P. santarosense*.

319 Phylogenetic studies of the genera of the Calamoideae show disparate results (*e.g.*, Thomas &  
320 De Franceschi, 2013; Thomas & Boura, 2015; Baker *et al.*, 2009; Kuhnhäuser *et al.*, 2021),  
321 and thus it is unclear if the presence of two vessels in the fvbs of the CZ and one in the SZ is  
322 a plesiomorphic condition of the clade (or some of the tribes within), or if it is sparsely  
323 widespread. The genera *Eugeissona*, *Mauritia* and *Raphia* have phytoliths restricted to the  
324 subcortical zone near the cortical region, while *Corypha*-type stems as *Palmoxylon*  
325 *santarosense* have phytoliths also in the CZ (Thomas & De Franceschi, 2013). Also, these  
326 genera also exhibit radial differentiation of the fibrous part (Thomas & De Franceschi, 2013),  
327 absent in the fossil taxon.

328 Among Arecoideae, the presence of two wide metaxylem elements in the fvbs of the CZ and  
329 one in the SZ is distributed across the phylogeny of the clade (see Thomas & Boura, 2015),  
330 probably reflecting multiple origins of the character. While most of the characters observed in  
331 the studied specimens are present in the clade, no genera have been reported exhibiting a  
332 *Corypha*-type stem (Thomas, 2011b). Nevertheless, it is worth mentioning that Arecoideae  
333 are a highly diverse family with unknown information regarding the anatomy of the stem of  
334 many of its representatives (Thomas, 2011b), and thus comparisons are difficult to make.

335 In summary, characters present in *Palmoxylon santarosense* are not exclusively present in  
336 any modern representative of the Areceaceae. As a result, it is here considered as an Areceaceae  
337 *incertae sedis*.

338

339 *Palmoxylon rionegrense* Ancibor 1995 *emend.* Vera

340 Figures 4–5

341 1995. *Palmoxylon rionegrense* Ancibor, *pro parte*. *Ameghiniana* 32(3): 298, Plate III A, D, H

342 **Type specimen.** BA Pb 884 (BA Pb Pm 263, 264, 265)

343 **Geographic occurrence.** Estancia El Palenque, 10 km west of Santa Rosa locality and 60 km  
344 northwestern to Nahuel Niyeu, Río Negro Province, Argentina, at a site named “Cañadón de  
345 Marcelo” (Bosque 2).

346 **Stratigraphic occurrence.** Allen Formation; Upper Cretaceous (upper Campanian to  
347 Maastrichtian).

348 **Original diagnosis (translated from Ancibor (1995), originally in spanish).** Radially  
349 extended fibrovascular bundles; 4–6 metaxylem vessels per fibrovascular bundle; large-  
350 lumen fibers with dark contents forming a cap only on the phloem side; phloem in 3–4  
351 strands; interfascicular parenchyma with thickened walls and no particular arrangement;  
352 Siliceous corpuscles are irregular and subspherical with marked spicules.

353 **Emended diagnosis.** Stem atactostelic. Central zone with ground tissue composed of slightly  
354 elongate to rod-like, thin walled cells constituting a compact tissue with few lacunae; fibrous  
355 bundles absent; growth pattern *Corypha*-type; density of fvbs in the CZ c. 190–240 per cm<sup>2</sup>;

356 f/v ratio c. 6–12 in the CZ; fvbs with dcap Reniforma in shape, with rounded median sinus;  
357 vcap present, exhibiting 1–2 layers of radially elongate fibers, tabular parenchyma present,  
358 radiating parenchyma absent; xylem part excluded, presenting 2 (range 2 to 4) wide  
359 metaxylem vessels and paravascular parenchyma poorly developed; presence of globular  
360 echinate and conical phytoliths in axial series of stigmata at the margins of the fibrous part of  
361 the fvbs.

362 **Description.** The description is based on the holotype specimen BA Pb 884, consisting of a  
363 sectioned fragment of stem c. 7.6 cm in maximum width and c. 1 cm tall (Fig. 4A). fvbs tend  
364 to have variable orientation, although there is some tendency to show a general arrangement  
365 with the dcap pointing to one of the margins of the stem in the region which was not  
366 sectioned (Fig. 4B–E), and a more irregular distribution towards the center/sectioned portion.  
367 As such, it is here interpreted as representing the central region of the CZ, with the portion  
368 where fvbs are more irregularly distributed as the most central region of CZ. Subcortical or  
369 CT are not preserved (Fig. 4C). Internally, it consists of parenchymatous ground tissue and  
370 scattered fvbs, arranged in an atactostele.

371 **Stem.** The density of fvbs in the most internal zone is 190–240 per cm<sup>2</sup>. Density in the most  
372 external zone preserved is 225–235 per cm<sup>2</sup>. Measured f/v ratio for fvbs is 6–12 in the most  
373 internal zone and 7–11 in the most external zone (Fig. 4C).

374 Organization and distribution of fvbs is regular throughout the preserved regions of the  
375 transverse section. The absence of preserved SZ or TZ zones, the similar values of density of  
376 fvbs and f/v ratio in the central and periphery of the preserved portion suggest that all the  
377 preserved portion represents the CZ of the stem. Presence of highly elongated parenchyma  
378 cells conforming the ground tissue is interpreted as evidence of ground parenchyma sustained  
379 growth (Fig. 4K), present in *Corypha*-type and *Mauritia*-type stems (Thomas & De

380 Franceschi, 2013). *Mauritia*-type stems have highly reduced fibrous portions of the fvbs in  
381 the CZ (Thomas & De Franceschi, 2013). As the dcaps are highly developed in this central  
382 portion of the studied fossil (with f/v values between 6 and 12), the stem is interpreted as  
383 having a *Corypha*-type growth pattern.

384 **Fibrovascular bundles.** Fibrovascular bundles typically exhibit the vascular portion with  
385 different grades of deformation (Fig. 4D–G), interpreted as the result of the elongation of  
386 parenchyma cells of the ground tissue. Description of the fvbs is based on the ones that show  
387 less deformation.

388 Fibrovascular bundles are 685–915 ( $794\pm 79$ )  $\mu\text{m}$  tall and 488–937 ( $654\pm 135$ )  $\mu\text{m}$  wide, being  
389 the ones located in the most central region slightly wider than the ones located at the  
390 periphery (Fig. 4D–G). Tabular parenchyma present, consisting of apparently 2 layers of  
391 elongate cells (Fig. 4F, G, K). Radiating parenchyma absent. Fibrous part Reniforma in shape  
392 (Stenzel, 1904), with absent to slightly rounded auricular sinuses. Median sinus rounded.  
393 Dorsal cap 343–625 ( $510\pm 65$ )  $\mu\text{m}$  high, composed of a dense mass of fibers (Fig. 4D–G).  
394 Fibers 16.2–50.6 ( $34\pm 9.3$ )  $\mu\text{m}$  in diameter, with thick walls, and showing a tendency of radial  
395 elongation towards the margin of the dcap, not observed in the marginal row of fibres (Fig.  
396 4F, G). Ventral cap present, crescentiform, composed of cells 11–21.1 ( $15.2\pm 3.2$ )  $\mu\text{m}$  in  
397 diameter, thick walled, often connecting with dcap (Fig. 4F–J). The xylem part of the  
398 fibrovascular bundles consist of typically 2 (rarely 1–4) included wide metaxylem elements  
399 51.7–111 ( $77.4\pm 16.1$ )  $\mu\text{m}$  in diameter (Fig. 4E–J); paravascular parenchyma poorly  
400 developed. Protoxylem and phloem regions are difficult to describe due to compression of the  
401 fvbs and preservation quality (Fig. 4H–J).

402 **Ground tissue.** Ground tissue is essentially parenchymatous, mostly composed of elongate to  
403 rod-like, thin walled cells (Fig. 4K), 32.8–111.9 ( $75.6\pm 26.6$ )  $\mu\text{m}$  in the longest axis and 18.7–

404 37.4 (27.6±6.7) µm in the shortest axis (length/width ratio 0.9–5.4), constituting a compact  
405 tissue with few lacunae, identified in longitudinal section (Fig. 5E). Fibrous bundles are not  
406 present in the ground tissue.

407 **Phytoliths.** In the longitudinal section, globular phytoliths 8.2–13.2 (10.8±2.1) µm in  
408 diameter (Fig. 5E), along with conical phytoliths 13.1–26.1 (18.8±4.3) µm tall and 10.8–18.4  
409 (15.3±2.6) µm wide (Fig. 5F, G), are present in stigmata in the marginal region of the fibrous  
410 part of the fvbs.

411 **Leaf traces.** Some bundles with fibrous and vascular components differ in their structure and  
412 size from the typical fvbs, and are interpreted as leaf traces. They are 865–1024 (945±111)  
413 µm tall and 999–1032 (1015±23) µm wide (Fig. 5A, B). Leaf traces are two-parted. The  
414 largest unit consists of a fibrous dcap similar to a Complanata to Reniforma shape, but with  
415 rounded auricular sinuses, and a central region exhibiting several (7–9) adjacent metaxylem  
416 vessels and probably unpreserved phloem (Fig. 5A–C). The second unit, separated from the  
417 first one by ground tissue, is a circular structure exhibiting numerous (20?) isolated  
418 metaxylem vessels arranged in an apparent circle (Fig. 5A–C).

419 **Vascular bridges.** Small fvbs are present in the ground tissue, adjacent (and opposite  
420 oriented) to leaf traces. They are c. 368 µm tall and 328.4 µm wide. They show an anatomy  
421 comparable to the one observed in the fvbs of the CZ, but have a dcap similar or smaller in  
422 size than the vascular part (Fig. 5A, D).

423 **Cortical zone.** Not preserved.

424 **Remarks.** Specimen BA Pb 898, originally included by Ancibor (1995) in this species is here  
425 referred to *P. valchetense* (see below).

426 **Comparisons with fossil forms from South America.** *Palmoxylon rionegrense* differs from  
427 *P. santarosense* by presenting ground tissue composed of highly elongate cells (Fig. 4K),  
428 fvbs in the central zone having a Reniforma type of fibrous part (Fig. 4D–G), and higher  
429 values of f/v ratio, resulting in fvbs with a fibrous part proportionally more developed than in  
430 the taxon described above. Additionally, only globular phytolits were identified in *P.*  
431 *santarosense*, while *P. rionegrense* also exhibits conical phytolits (Fig. 5F, G). To date, the  
432 Danian *P. patagonicum* is the only other *Palmoxylon* species reported from South America  
433 containing conical phytoliths (Table 1), but the Danian species has radiating parenchyma  
434 (absent in *P. rionegrense*) and contrasting low density of fvbs in the central zone, 14.5 per  
435 cm<sup>2</sup> vs 190–240 per cm<sup>2</sup> (Romero, 1968).

436 Among other *Palmoxylon* recorded from South America, several species exhibit values close  
437 to 2(2–4) wide metaxylem elements in the fvbs and ground parenchyma with elongate to rod-  
438 like cells (Table 1). *Palmoxylon garridoi* and *Palmoxylon* sp. 1 in Vera *et al.* (2024) differ  
439 from *P. rionegrense* by having fvbs without a developed vcap (Martínez, 2012; Vera *et al.*,  
440 2024). The remaining one, *P. subantarcticae*, is closely comparable to the specimen here  
441 studied. Martínez *et al.* (2023) reported fibrous bundles commonly present in the central zone  
442 of the stems of this species, and could be a difference from *P. rionegrense*, which lacks these  
443 structures. Other comparative characters, such as density of fvbs in different regions of the  
444 stem, and f/v values are not reported for *P. subantarcticae*, and may be a potentially relevant  
445 source of information to evaluate the similarities between these two taxa. In any case, conical  
446 phytoliths were unreported in *P. subantarcticae* (Martínez *et al.*, 2023, Table 1).

447 **Comparisons with extant taxa and affinities.** Few extant Arecaceae exhibit phytoliths that  
448 are not exclusively globose, and are included in the Arecoidea, the genus *Nypa* Steck, and the  
449 Caryoteae tribe of the Coryphoidea (Thomas, 2011a, b; Thomas & De Franceschi, 2013).

450 Arecoid palms typically exhibit 2 wide metaxylem elements in the CZ, changing to 1 in the  
451 SZ (Thomas, 2011a, b). While the SZ and the CT are unknown for *P. rionegrense*, it is  
452 noteworthy that fvbs have typically 2 or more wide metaxylem elements, and even in the  
453 outermost preserved regions of the stem fvbs with a single wide metaxylem element are not  
454 present. *Nypa*, sole extant representative of the Nypoidea, has a very reduced fibrous portion  
455 of the fvbs, with f/v ratio close to 1 (Thomas, 2011b), while the studied specimen exhibits f/v  
456 values of 6–12. The number of wide metaxylem elements in *P. rionegrense* is more  
457 comparable to the typical configuration of many Coryphoideae (Thomas, 2011b; Thomas &  
458 De Franceschi, 2013). Noteworthy, taxa exhibiting non-globular phytoliths among  
459 Coryphoidea have a comparable number of wide metaxylem elements per fvb to Arecoideae,  
460 i.e. 2 in CZ and 1 in SZ ((Thomas, 2011a, b; Thomas & De Franceschi, 2013). Nevertheless,  
461 phylogenetic studies on Coryphoideae suggest that this character state is a synapomorphy of  
462 the Caryoteae, while the plesiomorphic condition is fvbs with typically 2 wide metaxylem  
463 elements (see phylogeny in Kadam *et al.*, 2023, and character mapping in Thomas & Boura,  
464 2015). As a result, *P. rionegrense* may represent a stem of tribe Caryoteae, or a Coryphoid  
465 taxon related to the lineage that gave origin to the Caryoteae.

466

467 *Palmoxylon valchetense* Ancibor 1995 *emend.* Vera

468 Figures 6–7

469 1995. *Palmoxylon rionegrense* Ancibor, *pro parte*. *Ameghiniana* 32(3): 298, Plate III B, E, I

470 1995. *Palmoxylon valchetense* Ancibor. *Ameghiniana* 32(3): 298, Plate IV A-F

471 **Holotype.** BA Pb 890 (BA Pb Pm 257, 258, 259, 260, 261, 262)

472 **Epitype here designed.** BA Pb 967

473 **Additional specimens.** BA Pb 888, 889

474 **Geographic occurrence.** Estancia El Palenque, 10 km west of Santa Rosa locality and 60 km  
475 northwestern to Nahuel Niyeu, Río Negro Province, Argentina, at a site named “Cañadón de  
476 Marcelo” (Bosque 2).

477 **Stratigraphic occurrence.** Allen Formation; Upper Cretaceous (upper Campanian to  
478 Maastrichtian).

479 **Original diagnosis (translated from Ancibor (1995), originally in Spanish).** Skull-shaped  
480 slightly elongate fibrovascular bundles; 1–3 metaxylem vessels per fibrovascular bundle;  
481 Fibers with large lumina and variable size, forming a voluminous cap on the phloem side and  
482 arranged radially on the xylem side. Interfascicular parenchyma arranged perpendicular to the  
483 fibrovascular bundles in the longitudinal section. Phloem in two strands. Siliceous corpuscles  
484 sub-spherical to oval, eventually spiculated.

485 **Emended diagnosis.** Stem atactostelic, divided in CZ, SZ and CT. Ground tissue composed  
486 of isodiametric parenchymatous cells without lacunae, and sparse interspersed fibrous  
487 bundles in the CZ, and more abundant towards the periphery of the stem; growth pattern  
488 *Cocos*-type; density of fvbs in the CZ c. 14–17 per cm<sup>2</sup> and in the SZ is c. 77–84 per cm<sup>2</sup>; f/v  
489 ratio c. 3–4 in the most internal zone of CZ and c. 3.3–7.7 in the most external region of the  
490 SZ; fvbs with dcap Reniforma in shape, with rounded median sinus; vcap present, exhibiting  
491 1–2 layers of radially elongate fibers, tabular parenchyma present, radiating parenchyma  
492 absent; phloem undivided to presenting a partition resulting from ventral projection of the  
493 dcap; xylem part excluded, presenting 2 (range 1 to 4) wide metaxylem vessels and

494 developed paravascular parenchyma; presence of globular echinate phytoliths in axial series  
495 of stegmata at the margins of the fibrous bundles and fibrous part of the fvbs.

496 **Description.** The description is based on four specimens. The holotype BA Pb 890 is a  
497 narrow sectioned fragment of stem, c. 7.6 cm in maximum width and c. 1 cm tall (Fig. 6A).  
498 The specimen exhibits only a small transverse section, containing less than 50 vascular  
499 bundles (between fvbs and leaf traces). The second specimen referred to Ancibor (1995), BA  
500 Pb 888 agrees in the anatomy of the fvbs of the holotype, but shows a small portion with  
501 smaller fvbs (Fig. 6B). A third specimen, BA Pb 967 is a large stem showing variable  
502 changing density and size of the fvbs in cross section (Fig. 6D), and is referred to this species,  
503 allowing the recognition of BA Pb 890 as portion of the CZ, and BA Pb 888 as part of the  
504 region between the CZ and TZ. Finally, BA Pb 898 (Fig. 6C) was originally referred to *P.*  
505 *rionegrense* by Ancibor (1995), but is here interpreted as a portion of the TZ of the stem of *P.*  
506 *valchetense*, due to overlapping features with BA Pb 967 of the size, shape and anatomy of  
507 the fvbs (Fig. 6F–J).

508 **Stem.** The density of fvbs in the center of the CZ is 14–17 per cm<sup>2</sup>. Density in the most  
509 external preserved region of the SZ is 77–84 per cm<sup>2</sup> (Fig. 6D, E). Ratio of density of fvbs in  
510 the SZ vs density in the CZ c. 5.1. Measured f/v for fvbs is 3–4 in the most internal zone of  
511 the CZ ( $f/v_{in}$ ) and 3.7–7.7 in the most external region of the SZ ( $f/v_{out}$ ). Ratio between  $f/v_{out}$  /  
512  $f/v_{in}$  c. 1.6. Fibrous covering index is 0.17–0.18 in the most internal zone of the CZ ( $FCI_{in}$ )  
513 and 0.38–0.44 in the SZ ( $FCI_{out}$ ). Ratio between  $FCI_{out}$  and  $FCI_{in}$  is 2.35. All these  
514 parameters, along with the absence of tangential differentiation of the fibrous part of the fvbs,  
515 are in agreement with a *Cocos*-type growth pattern (von Mohl, 1823–1850; Thomas & De  
516 Franceschi, 2013).

517 **Fibrovascular bundles.** Fibrovascular bundles of the CZ are 1574.4–2129.3 (1840.6±182.5)  
518 µm tall and 1654.4–2025.7 (1794.8±139.8) µm wide (Fig. 6F–H). Tabular parenchyma  
519 present, consisting of 2-3 layers of elongate cells (Fig. 6L). Radiating parenchyma absent.  
520 Fibrous part Reniforma in shape (Stenzel, 1904) (Fig. 6F–H), with absent to angular auricular  
521 sinuses. Median sinus slightly rounded to rounded. Dorsal cap 886–1162.5 (1006.8±117.7)  
522 µm high, composed of a dense mass of fibers. Fibers 16.1–75.2 (37.5±18.4) µm in diameter,  
523 polygonal to slightly elongate (towards the margin of the dcap) with thick walls (Fig. 6L).  
524 Ventral cap present, crescentiform, connecting with the dcap, often exhibiting a projection  
525 towards the xylem (Fig. 6F–H, 7A–D). Ventral cap composed of 1–3 layers of isodiametric to  
526 polygonal cells 11.1–34.2 (23.2±6.3) µm in diameter, adjacent to the xylem portion, and a  
527 single (rarely two), layers of rectangular radiating cells, 26.8–80 (55.8±15.6) µm long and  
528 19–29.4 (24.7±3.9) µm wide (Fig. 7A–D), similar to radiating parenchyma. The xylem part of  
529 the fibrovascular bundles consist of typically 2 (range 2–4) excluded wide metaxylem  
530 elements 65.3–191.1 (137.2±39.2) µm in diameter (Fig. 6F–H, 7A–D); paravascular  
531 parenchyma highly developed (Fig. 7A–D). Protoxylem elements (and small metaxylem  
532 elements?) interspersed in the paravascular parenchyma between larger metaxylem vessels,  
533 32.3–70.2 (49.1±13.8) µm in diameter, typically present in fvbs with 2 wide metaxylem  
534 elements (Fig. 7D). Phloem typically consists of a single strand, although several fvbs show a  
535 partition produced by a ventral projection of the dcap, dividing the phloem in two strands.  
536 Sieve cells 15.2–47.8 (28.9±9.4) µm in diameter (Fig. 7A, C); metaphloem sieve plate not  
537 observed.

538 Towards the SZ, fvbs become smaller, 795.3–995.4 (901.5±85.5) µm tall and 981.6–1140.2  
539 (1058.7±57.6) µm wide, retaining the characteristics of the ones present in the CZ. This  
540 change in size is somewhat abrupt, having 1 or 2 “transitional fvbs” between the larger ones  
541 of the CZ and the smaller of the SZ (Fig. 6I–K; 7E–G).

542 **Ground tissue.** Ground tissue is essentially parenchymatous, mostly composed of  
543 isodiametric, spheroidal to slightly elongate parenchymatous cells, 17.4–55.1 (30.7±10.7) µm  
544 in diameter, constituting a compact tissue without lacunae or intercellular spaces (Fig. 7I–K).  
545 Parenchymatous cells of the ground tissue in the holotype (BA Pb 890) exhibit thickened  
546 walls (Fig. 7I).

547 Fibrous bundles in the CZ are typically sparse and small, 66.8–91.8 (75.9±9.6) µm in  
548 diameter (Fig. 7J). In the SZ and the CT, larger fibrous bundles are also present, being more  
549 abundant than the ones in the CZ (Fig. 7G, H, J, K) . These bundles are circular to oval in  
550 cross section, 63.6–196.5 (158.4±31.3) µm in diameter.

551 **Phytoliths.** In the longitudinal section, globular granulate phytoliths 8.6–15.3 (11.5±1.8) µm  
552 in diameter are present in stigmata in the marginal region of the fibrous part of the fvbs (Fig.  
553 7O).

554 **Leaf traces.** Interspersed between fvbs are some slightly larger bundles exhibiting a vascular  
555 portion proportionally smaller and slightly rounded to absent median sinus, but otherwise  
556 comparable to fvbs, interpreted as leaf traces (Fig. 7L). Leaf traces are 1368–1730  
557 (1539±160) tall and 1795–2080 (1908±151) wide (Fig. 7L–M).

558 **Vascular bridges.** Several small bundles are present in the ground tissue, typically adjacent  
559 (and opposite oriented) to leaf traces (Fig. 7L). They are 257–539 (413±116.) µm tall and  
560 288–446 (348±68) µm wide, exhibiting an anatomy comparable to the one observed in the  
561 fvbs, but having a proportionally smaller dcap, morphologically close to *Lunaria* in shape  
562 (Fig. 7N).

563 **Cortical zone.** Only a very small portion interpreted as belonging to the cortex is preserved  
564 in BA Pb 967. It differs from the underlying zone by having lower density of fvbs, abundant

565 fibrous bundles, and fvbs exhibiting slightly elongate dcaps (Fig. 6K, 7H). Measured  
566 thickness of the cortical zone is at least 1 mm.

567 **Remarks.** The holotype specimen (BA Pb 890) selected by Ancibor (1995) only preserves a  
568 small portion of the CZ of the stem, while the specimen BA Pb 888, originally included by  
569 the author in the species (Ancibor, 1995), provides more information regarding the structure  
570 and distribution of the fvbs in the stem, exhibiting a small portion of the SZ, and would  
571 probably have been a better holotype for the species. Nevertheless, the inclusion in this  
572 species of BA Pb 967, the most complete specimen available to date of the species (collected  
573 after Ancibor's contribution), allows a more comprehensive interpretation of this taxon, as  
574 well as the recognition of BA Pb 898 (originally referred to *P. rionegrense*) as another  
575 sample belonging to *P. valchetense*. To allow an amendment of the diagnosis of the species  
576 and clarify its taxonomic limits, BA Pb 967 is selected as an epitype of *Palmoxylon*  
577 *valchetense* (ICN Art. 9.9).

578 Thick walled parenchyma cells near composing the ground tissue of the holotype probably  
579 reflect a mature condition of the tissue, indicating a provenance of the sample near the base  
580 of the stem (Thomas & De Franceschi, 2013).

581 **Comparisons with fossil forms from South America.** *Palmoxylon valchetense* can be  
582 separated from *P. santarosense* by having 2(1–4) wide metaxylem vessels per fvb (Fig. 6F–  
583 K), contrasting with the 2 vessels in the CZ and 1 in the SZ in the latter taxon, as well as by  
584 the presence of divided phloem strands in *P. valchetense*, (Fig. 7A, C) absent in *P.*  
585 *santarosense*. *Palmoxylon valchetense* differs from *P. rionegrense* by having typically  
586 isodiametric to slightly elongate parenchyma ground cells (Fig. 7I), while *P. rionegrense* has  
587 elongate to rod-like cells. In the latter species, f/v ratio is 6–12 in the CZ, while in *P.*

588 *valchetense* this value is lower (3–4). *P. rionegrense* also lacks elongate cells forming the  
589 vcap.

590 Two species of *Palmoxylon* reported from the region (*P. patagonicum* and *P. vaterum*)  
591 exhibit 2(1–4) wide metaxylem elements per fvb and two phloem strands produced by the  
592 projection of the dcap (Table 1). *Palmoxylon patagonicum* has abundant fibrous bundles in  
593 the central region of the stem (Romero, 1968), contrasting with the scarce number reported in  
594 *P. valchetense*. Additionally, *P. patagonicum* has radiating parenchyma and conical phytoliths  
595 (Table 1), absent in the species here described. On the other hand, *P. vaterum* has fvbs with a  
596 dcap exhibiting a Vaginata shape, contrasting with the Reniforma shape observed in *P.*  
597 *valchetense* (Fig. 6F–J). A species that has unpreserved phloem but has a similar number of  
598 wide metaxylem elements per fvbs is *Palmoxylon bororoense*, but it is also characterized by  
599 having fvbs with a dcap Vaginata in shape (Table 1).

600 **Comparisons with extant taxa and affinities.** The presence of fvbs with a sclerotic partition  
601 of the phloem as a result of a ventral projection of the dcap, in combination with a vcap, are  
602 typically found in the tribe Trachycarpeae of the Coryphoideae (Thomas & De Franceschi,  
603 2013). Genera within this tribe also exhibiting a dcap Reniforma in shape and 2(3–4) wide  
604 metaxylem elements per fvb include *Serenoa* Hook.f., *Brahea* Mart. ex. Endl., *Copernicia*  
605 Mart., *Pritchardia* Seem. et H. Wendl., *Licuala* Thunb. and *Livistona* R. Br. of the  
606 Livistoninae, and *Rhaphis* of the Rhaphidinae (Thomas, 2011a, b; Thomas & De Franceschi,  
607 2013). Other features recorded in *P. valchetense*, as the *Cocos*-type stem, are also present in  
608 some of the trachycarpeoid genera (see Thomas & De Franceschi, 2013), supporting its  
609 referral to this tribe.

610

611 **Discussion**

612 ***Palmoxylon* species from the Allen Formation.** The restudy of the *Palmoxylon* species from  
613 the Allen Formation allows for a more complete characterization of each taxon and its limits.  
614 The inclusion of unpublished remains, together with a reevaluation of the originally described  
615 specimens, resulted in the recognition of characters unreported by Ancibor (1995), such as  
616 the growth pattern types and other descriptors currently used in modern characterization of  
617 living and extinct palm stems (e.g., Thomas & De Franceschi, 2012, 2013; Franco *et al.*,  
618 2014; Vera *et al.*, 2024; Kumar *et al.*, 2025). Consequently, the diagnoses of the three species  
619 were emended to incorporate these newly recognized features, and to modify some characters  
620 that are interpreted differently in this contribution.

621 In this study, epitypes for *Palmoxylon santarosense* and *Palmoxylon valchetense* are  
622 designated. This procedure was necessary because the selected specimens provide  
623 information beyond that obtainable from small stem fragments: they allow a comprehensive  
624 interpretation of the growth type and structural changes within the stems. The holotypes  
625 selected by Ancibor (1995) consist of limited stem portions where this information was not  
626 available. For the remaining species, *Palmoxylon rionegrense*, however, only the holotype is  
627 available, and thus no epitype was defined.

628 The new descriptions presented here show several differences from those of Ancibor (1995),  
629 which have been widely used in comparisons with other *Palmoxylon* taxa (e.g., Martínez,  
630 2012; Martínez *et al.*, 2023; Vera *et al.*, 2024); therefore, the revised anatomical data from  
631 the Allen Formation palms provide a more robust basis for interspecific and interbasinal  
632 comparisons, highlighting the importance of the restudy of previously published taxa. In  
633 particular, the incorporation of patterns of distribution of fvbs, as well of the anatomical  
634 changes of these structures across the different sections of the stem, were barely mentioned in  
635 the original descriptions (Ancibor, 1995), and are currently included in the descriptive traits

636 that allow characterizing the anatomy of palm stems (*e.g.*, Thomas and De Franceschi, 2013).  
637 Moreover, these descriptions offer insights not only into anatomical and taxonomic affinities  
638 but also into the broader paleoecological significance of these taxa.

639 Recognizing the affinities of the Allen Formation *Palmoxylon* species is also critical for  
640 evaluating their potential use as paleoclimatic proxies. Among the studied taxa, *Palmoxylon*  
641 *santarosense* proves to be the least informative, as it shows a combination of characters not  
642 observed in extant Arecaceae, and thus precluding its referral to any specific subfamily or  
643 tribe within Arecaceae. In contrast, *Palmoxylon rionegrense*, although based in a single  
644 specimen, has enough anatomical information to warrant its referral to the Coryphoideae, a  
645 clade currently restricted to environments with mean annual temperatures (MAT) of 8.9–30  
646 °C (Reichgelt *et al.*, 2018). Tentative affinities with the tribe Caryoteae are also suggested,  
647 which would imply a narrower MAT range of 15.3–27.4 °C (Reichgelt *et al.*, 2018). Finally,  
648 *Palmoxylon valchetense* is now interpreted as belonging to the tribe Trachycarpeae, which is  
649 associated with MAT values of 8.2–29.4 °C (Reichgelt *et al.*, 2018). As discussed below, the  
650 record of latest Cretaceous palms with affinities with the Trachycarpeae also provide  
651 information regarding the biogeography of the clade. In summary, while tropical conditions  
652 for the Allen Formation are not rejected, these results indicate that the three palms described  
653 herein are not, at least for the time being, biological proxies supporting (or challenging) these  
654 climatic conditions.

655

656 **Comments on biogeography of Trachycarpeae.** The Trachycarpeae has one of the largest  
657 geographic distributions among Arecaceae, being present in tropical North and Central  
658 America, some regions of central South America, the Mediterranean region, and Australasia  
659 (Dransfield *et al.*, 2008). Bacon *et al.* (2012) postulated that the origin of the clade

660 Trachycarpeae occurred during the Coniacian–Santonian in a region spanning southern North  
661 America, Central America and the Caribbean, and that crown-Trachycarpeae appeared during  
662 the Eocene–Oligocene, diversifying mostly during the Miocene. Baker and Couvreur (2013),  
663 while obtaining a similar geographic origin, recovered the divergence of the clade during  
664 more recent times (during the Eocene).

665 Kumar *et al.* (2025) recently described the species *Palmoxylon trachycarpeaeense* Kumar et  
666 Khan 2025 from the Maastrichtian–Danian Deccan Intertrappean Beds in India, interpreting it  
667 as a representative of the Trachycarpeae. This record, along with younger palm fossils from  
668 the region with Trachycarpean affinities, allowed the authors to challenge hypothesis of a  
669 Laurasian origin for the tribe made by Bacon *et al.* (2012) and Baker and Couvreur (2013),  
670 suggesting that this clade originated in the gondwanan fragment that is India today, after its  
671 separation from Antarctica but before its accretion with Laurasia (Kumar *et al.*, 2025).

672 Anatomical characters of *Palmoxylon trachycarpeaeense* show close similarities with  
673 *Copernicia* and *Washingtonia* of the Trachycarpeae when included in the Thomas (2011a)  
674 Database, highlighting the probable relationship with this tribe. Nevertheless, another taxon is  
675 recovered as comparable: the Sabaleae. In fact, anatomical studies focused on descriptive  
676 characters carried out by Thomas (2011a, b) and Thomas and De Franceschi (2013) recover  
677 the Sabaleae as indistinguishable from these two Trachycarpeoid genera when the defined  
678 descriptors are analyzed. Kumar *et al.* (2025) separate *P. trachycarpeaeense* from the  
679 Sabaleae indicating that fvbs of both taxa differ in shape and size, without indicating which  
680 are these differences in the shape, or which measurements of the fvbs taken into account for  
681 the Sabaleae (and its source). However, photographs of fvbs of the species of *Sabal* presented  
682 by Thomas (2011b) show, a priori, fvbs similar regarding the morphology and size. It is  
683 unclear which morphological differences were recognized by Kumar *et al.* (2025) to  
684 segregate the studied *Palmoxylon* species from Sabaleae. As such, while affinities with the

685 Trachycarpeae cannot be rejected, restricting it to this tribe may be obscuring possible  
686 affinities with the Sabaleae.  
687 While the gondwanan record of *Palmoxylon trachycarpeaeense* may or may not challenge the  
688 laurasian origin of the clade, the recognized Trachycarpeae affinities of *Palmoxylon*  
689 *valchetense* from the Allen Formation of Patagonia may add a new line of evidence  
690 supporting a role of the gondwanan realm in the early history of the Trachycarpeae during the  
691 Cretaceous. Interestingly, *Palmoxylon subantarcticae* from the uppermost Cretaceous  
692 Dorotea Formation from Chile also shares similarities with the Trachycarpeae and Sabaleae  
693 (Martínez *et al.*, 2023). In this sense, accepting these Patagonian species as true  
694 representatives of the tribe clashes with the molecular divergence estimations carried out by  
695 Baker and Couvreur (2013), but may agree with the ones proposed by Bacon *et al.* (2012) for  
696 the stem representatives of the clade. In any case, these palm fossils seem to occur earlier in  
697 the history of palms than estimated by molecular clocks. Similarly, Chate *et al.* (2019) and  
698 Vera *et al.* (2024) reported uppermost Cretaceous to Danian fossils closely comparable to the  
699 tribe Phytelephea of the subfamily Ceroxyloidea from India and Patagonia respectively,  
700 predating by more than 20 My the estimated divergence time of the clade (Baker & Couvreur,  
701 2013; Chate *et al.*, 2019; Khan *et al.*, 2020; Vera *et al.*, 2024). It is clear that future studies on  
702 Arecaceae, incorporating more fossils with conclusive affinities as calibration points may  
703 produce divergence time estimates concordant with what is already known by different fossil  
704 specimens, and allow the proposal of new dispersal patterns supported by the already rich  
705 known palm fossil record.

706

## 707 **Conclusions**

708

709 The three *Palmoxylon* species originally described by Ancibor (1995) from the Campanian–  
710 Maastrichtian Allen Formation (Río Negro Province, Argentina) are restudied here. The new  
711 descriptions incorporate additional anatomical data and allowed revised diagnoses. New  
712 unpublished material is referred to one of these species, and epitypes are designated for  
713 *Palmoxylon santarosense* and *Palmoxylon valchetense*, based on the more comprehensive  
714 anatomical information they provide.

715 This study also establishes new taxonomic affinities for the three taxa. The anatomy of *P.*  
716 *santarosense* is not diagnostic enough to confidently assign it to any subfamily or tribe within  
717 Arecaceae and is therefore referred to Arecaceae *incertae sedis*. In contrast, *P. rionegrense* is  
718 interpreted as belonging to the subfamily Coryphoideae, with probable affinities to the tribe  
719 Caryoteae, while *P. valchetense* is recognized as a member of the tribe Trachycarpeae. Given  
720 the broad climatic tolerances of these clades, their occurrence does not provide conclusive  
721 support for, nor does it rule out, tropical climatic conditions for the Allen Formation.

722 The occurrence of Trachycarpeae in the latest Cretaceous of South America has important  
723 evolutionary and biogeographic implications. It challenges existing divergence time estimates  
724 for the clade and calls into question proposed biogeographic scenarios involving the  
725 Laurasian realm or India. These findings highlight the need to incorporate a greater number  
726 of fossil records into molecular clock calibrations and analyses of origin and dispersal, which  
727 are typically based on modern taxa and include few fossil calibration points.

728

## 729 **Acknowledgments**

730

731 Thanks are due to Dr. Georgina del Fueyo (MACN) and Luis Lezama (MACN) for allowing  
732 access to the specimens of *Palmoxylon* housed in the Colección Nacional de Paleobotánica

733 under their care, as well as sharing information regarding the fossils history. I also thank Dr.  
734 María Victoria Sánchez (MACN) for granting access to the specimen housed in the  
735 Colección Nacional de Icnología under her care. I am greatly indebted to Dr. Jorge Genise  
736 (MACN), who kindly shared their information regarding the fossiliferous site and the history  
737 of this finding, and allowed including a precise geographic provenance of the studied fossils.  
738 Dr. Leonardo Salgado (IIPG) pointed out the stratigraphic provenance of the fossils as well,  
739 and is also acknowledged. Thanks are extended to Editor Dr. Kelly Matsunaga, Reviewer  
740 Dra. Daniela P. Ruiz, and an anonymous reviewer, for their comments and suggestions that  
741 improved the final version of the manuscript. This work is a contribution to the National  
742 Geographic Society Project “The End of the Dinosaur Era in Patagonia” (NGS-92822R-22)  
743 granted to Dr. Diego Pol.

744

#### 745 **References**

746 Ancibor, E. (1995). Palmeras fósiles del Cretácico Tardío de la Patagonia argentina, Bajo de  
747 Santa Rosa, Río Negro. *Ameghiniana*, 32, 287–299.

748 Agnolín, F. L. (2010a). An avian coracoid from the Upper Cretaceous of Patagonia,  
749 Argentina. *Studia Geologica Salmanticensia*, 46(2), 99–119.

750 Agnolín, F. L. (2010b). A new species of the genus *Atlantoceratodus* (Dipnoiformes:  
751 Ceratodontoidei) from the uppermost Cretaceous of Patagonia and a brief overview of fossil  
752 dipnoans from the Cretaceous and Paleogene of South America. *Brazilian Geographical*  
753 *Journal: Geosciences and Humanities Research Medium*, 1, 162–210.

754 Agnolín, F. L. (2012). Una nueva Calyptocephalellidae (Anura, Neobatrachia) del Cretácico  
755 Superior de la Patagonia, Argentina, con comentarios sobre su posición sistemática. *Studia*  
756 *Geologica Salmanticensia*, 48, 129–178.

757 Agnolín, F. L., Aranciaga-Rolando, A. M., & Ortiz, R. (2025). New chelid turtle with a  
758 flattened skull from the Late Cretaceous of northern Patagonia, Argentina. *Alcheringa: An*  
759 *Australasian Journal of Palaeontology*, 49, 79–84.

760 <https://doi.org/10.1080/03115518.2024.2427261>

761 Agnolín, F. L., Powell, J. E., Novas, F. E., & Kundrát, M. (2012). New alvarezsaurid  
762 (Dinosauria, Theropoda) from uppermost Cretaceous of north-western Patagonia with  
763 associated eggs. *Cretaceous Research*, 35, 33–56.

764 <https://doi.org/10.1016/j.cretres.2011.11.014>

765 Álvarez Nogueira, R., Agnolín, F. L., Rozadilla, S., Aranciaga-Rolando, M., & Novas, F. E.  
766 (2025). Ankylosaurian remains from a new Campanian–Maastrichtian locality in Northern  
767 Patagonia, Argentina. *Alcheringa: An Australasian Journal of Palaeontology*, 49, 69–78.

768 <https://doi.org/10.1080/03115518.2025.2467462>

769 Andreis, R., Ancibor, E., Archangelsky, S., Artabe, A., Bonaparte, J., & Genise, J. (1991).  
770 Asociación de vegetales y animales en estratos del Cretácico tardío del norte de Patagonia.  
771 *Ameghiniana*, 28, 201–202.

772 Aranciaga Rolando, M., Cerroni, M. A., García Marsà, J. A., Agnolín, F. L., Motta, M. J.,  
773 Rozadilla, S., Brisson Eglí, F., & Novas, F. E. (2021). A new medium-sized abelisaurid  
774 (Theropoda, Dinosauria) from the late Cretaceous (Maastrichtian) Allen Formation of  
775 northern Patagonia, Argentina. *Journal of South American Earth Sciences*, 105, 102915.

776 <https://doi.org/10.1016/j.jsames.2020.102915>

777 Arguijo, M. H. (1979). *Palmoxylon bororoense* n. sp. de la Formación Cerro Bororó  
778 (Paleoceno), provincia de Chubut, Argentina. *Physis*, 38, 87–96.

779 Arguijo, M. H. (1981). *Palmoxylon vaterum*, n. sp. del Paleoceno (Daniano) de la provincia  
780 de Chubut, Argentina. *Physis*, 39, 49–59.

781 Artabe, A. E., Zamuner, A. B., & Stevenson, D. W. (2004). Two new petrified cycad stems,  
782 *Brunoa* gen. nov. and *Worsdellia* gen. nov., from the Cretaceous of Patagonia (Bajo de Santa  
783 Rosa, Río Negro Province), Argentina. *The Botanical Review*, 70, 121–133.  
784 [https://doi.org/10.1663/0006-8101\(2004\)070\[0121:TNPCSB\]2.0.CO;2](https://doi.org/10.1663/0006-8101(2004)070[0121:TNPCSB]2.0.CO;2)

785 Artabe, A. E., Zamuner, A. B., & Stevenson, D. W. (2005). A new genus of Late Cretaceous  
786 cycad stem from Argentina, with reappraisal of known forms. *Alcheringa: An Australasian*  
787 *Journal of Palaeontology*, 29, 87–100. <https://doi.org/10.1080/03115510508619561>

788 Bacon, C. D., Baker, W. J., & Simmons, M. P. (2012). Miocene dispersal drives island  
789 radiations in the palm Tribe Trachycarpeae (Arecaceae). *Systematic Biology*, 61, 426–442.  
790 <https://doi.org/10.1093/sysbio/syr123>

791 Baker, W. J., & Couvreur, T. L. P. (2013). Global biogeography and diversification of palms  
792 sheds light on the evolution of tropical lineages. I. Historical biogeography. *Journal of*  
793 *Biogeography*, 40, 274–285. <https://doi.org/10.1111/j.1365-2699.2012.02795.x>

794 Baker, W. J., Savolainen, V., Asmussen-Lange, C. B., Chase, M. W., Dransfield, J., Forest,  
795 F., Harley, M. M., Uhl, N. W., & Wilkinson, M. (2009). Complete generic-level phylogenetic  
796 analyses of palms (Arecaceae) with comparisons of supertree and supermatrix approaches.  
797 *Systematic Biology*, 58, 240–256. <https://doi.org/10.1093/sysbio/syp021>

798 Bogan, S., Taverne, L., & Agnolín, F. (2011). Description of a new aspidorhynchid fish,  
799 *Belonostomus lamarquensis* sp. nov. (Halecostomi, Aspidorhynchiformes), from the  
800 continental Upper Cretaceous of Patagonia, Argentina. *Bulletin de l'Institut Royal des*  
801 *Sciences Naturelles de Belgique, Sciences de la Terre*, 81, 5–16.

802 Chate, S. V., Bonde, S. D., & Gamre, P. G. (2019). *Palmoxylon phytelephantoides* sp. nov. A  
803 new fossil palm from the Deccan Intertrappean Beds of Umaria, Madhya Pradesh, India.  
804 *International Journal of Advanced Science Research and Management*, 4, 189–193.

805 Clarke, J. A., & Chiappe, L. M. (2001). A new carinate bird from the Late Cretaceous of  
806 Patagonia (Argentina). *American Museum Novitates*, 3323, 1–23.

807 Connelly, B. E., Cardozo, M. S., Montgomery, J. D., & Rougier, G. W. (2024). New  
808 mammals from the Upper Cretaceous Allen Formation (Patagonia, Argentina) and  
809 reassessment of meridiolestidan diversity. *Cretaceous Research*, 162, 105935.  
810 <https://doi.org/10.1016/j.cretres.2024.105935>

811 Cruzado Caballero, P., & Powell, J. (2017). *Bonapartesaurus rionegrensis*, a new  
812 hadrosaurine dinosaur from South America: Implications for phylogenetic and biogeographic  
813 relations with North America. *Journal of Vertebrate Paleontology*, 37, e1289381.  
814 <https://doi.org/10.1080/02724634.2017.1289381>

815 Del Fueyo, G. M. (1998). Coniferous woods from the Upper Cretaceous of Patagonia,  
816 Argentina. *Revista Española de Paleontología*, 13, 43–50.

817 Dransfield, J., Uhl, N. W., Asmussen, C. B., Baker, W. J., Harley, M. M., & Lewis, C. E.  
818 (2008). *Genera Palmarum: The evolution and classification of palms*. Royal Botanic  
819 Gardens, Kew.

820 Franco, M. J. (2014). Estípites de Arecaceae en la Formación Ituzaingó (Plioceno-  
821 Pleistoceno), Entre Ríos, Argentina. *Acta Geológica Lilloana*, 26, 14–29.

822 Franco, M. J., Brea, M., & Herbst, R. (2014). *Palmoxylon romeroi* sp. nov., de la Formación  
823 Chiquimil (Mioceno Superior) del Valle de Santa María, Provincia de Catamarca, Argentina.  
824 *Ameghiniana*, 51, 572–584. <https://doi.org/10.5710/AMGH.15.09.2014.2811>

825 Garberoglio, F. F., Gómez, R. O., Apesteguía, S., & Rougier, G. W. (2025). A Late  
826 Cretaceous lizard assemblage from the Allen Formation, northern Patagonia, Argentina.  
827 *Historical Biology*, 37, 950–962. <https://doi.org/10.1080/08912963.2024.2344789>

828 García, R., & Salgado, L. (2011). The titanosaur sauropods from the Allen Formation (late  
829 Campanian–early Maastrichtian) of Salitral Moreno (Patagonia, Río Negro, Argentina). *Acta*  
830 *Palaeontologica Polonica*, 56, 311–324. <https://doi.org/10.4202/app.2011.0055>

831 Genise, J. F. (1995). Upper Cretaceous trace fossils in permineralized plant remains from  
832 Patagonia, Argentina. *Ichnos: An International Journal for Plant and Animal Traces*, 3(4),  
833 287–299. <https://doi.org/10.1080/10420949509386399>

834 Genise, J. F., Garrouste, R., Nel, P., Grandcolas, P., Maurizot, P., Cluzel, D., Cornette, R.,  
835 Fabre, A.-C., & Nel, A. (2012). *Asthenopodichnium* in fossil wood: Different trace makers as  
836 indicators of different terrestrial palaeoenvironments. *Palaeogeography, Palaeoclimatology,*  
837 *Palaeoecology* 365–366, 184–191. <https://doi.org/10.1016/j.palaeo.2012.09.025>

838 Gómez, R. O. (2016). A new pipid frog from the Upper Cretaceous of Patagonia and early  
839 evolution of crown-group Pipidae. *Cretaceous Research*, 62, 52–64.  
840 <https://doi.org/10.1016/j.cretres.2016.02.006>

841 Kadam, S. K., Tamboli, A. S., Mane, R. N., Yadav, S. R., Choo, Y.-S., Burgos-Hernández,  
842 M., & Pak, J. H. (2023). Revised molecular phylogeny, global biogeography, and  
843 diversification of palms subfamily Coryphoideae (Arecaceae) based on low copy nuclear and

844 plastid regions. *Journal of Plant Research*, 136, 159–177. <https://doi.org/10.1007/s10265->  
845 [022-01425-5](https://doi.org/10.1007/s10265-022-01425-5)

846 Khan, M. A., Hazra, M., Mahato, S., Spicer, R. A., Roy, K., Hazra, T., Bandopadhaya, M.,  
847 Spicer, T. E. V., & Bera, S. (2020). A Cretaceous Gondwanan origin of the wax palm  
848 subfamily (Ceroxyloideae: Arecaceae) and its paleobiogeographic context. *Review of*  
849 *Palaeobotany and Palynology*, 283, 104318. <https://doi.org/10.1016/j.revpalbo.2020.104318>

850 Kuhnhäuser, B. G., Bellot, S., Couvreur, T. L. P., Dransfield, J., Henderson, A., Schley, R.,  
851 Chomicki, G., Eiserhardt, W. L., Hiscock, S. J., & Baker, W. J. (2021). A robust  
852 phylogenomic framework for the calamoid palms. *Molecular Phylogenetics and Evolution*,  
853 157, 107067. <https://doi.org/10.1016/j.ympev.2020.107067>

854 Kumar, S., Spicer, R. A., & Khan, M. A. (2025). Fossil evidence of Trachycarpeae  
855 (Arecaceae) from the K-Pg of India and its biogeographic implications. *Botany Letters*, 1–14.  
856 <https://doi.org/10.1080/23818107.2025.2502926>

857 Lutz, A. I. (1980). Descripción morfo–anatómica del estípite de *Palmoxylon concordiense*  
858 Lutz del Plioceno de la Pcia. de Entre Ríos, Argentina. *Facena*, 6, 17–32.

859 Lutz, A. I. (1984). *Palmoxylon yuqueriense* nov. sp. del Plioceno de la Pcia. de Entre Ríos,  
860 Argentina. En *Proceedings of the 3rd Congreso Argentino de Paleontología y*  
861 *Bioestratigrafía* (pp. 197–207). Corrientes, Argentina.

862 Lutz, A.I. (1986). Descripción morfo-anatómica del estípite de *Palmoxylon concordiense*  
863 Lutz del Plioceno de la provincia de Entre Rios, Argentina. *Facena* 6, 17–32.

864 Martínez, L. C. A. (2012). Estípites de palmera en el Campaniano del Grupo Neuquén,  
865 Provincia del Neuquén, Argentina. *Ameghiniana*, 49, 573–584.  
866 <https://doi.org/10.5710/AMGH.7.2.2012.514>

867 Martínez, L. C. A., Artabe, A. E., & Bodnar, J. (2012). A new cycad stem from the  
868 Cretaceous in Argentina and its phylogenetic relationships with other Cycadales: Cretaceous  
869 Patagonian Cycad Stem. *Botanical Journal of the Linnean Society*, 170, 436–458.  
870 <https://doi.org/10.1111/j.1095-8339.2012.01300.x>

871 Martínez, L. C. A., Leppe, M., Manríquez, L. M. E., Pino, J. P., Trevisan, C., Manfroi, J., &  
872 Mansilla, H. (2023). A unique Late Cretaceous fossil wood assemblage from Chilean  
873 Patagonia provides clues to a high-latitude continental environment. *Papers in*  
874 *Palaeontology*, 9, e1536. <https://doi.org/10.1002/spp2.1536>

875 Novas, F. E., Kundrát, M., Agnolín, F. L., Ezcurra, M. D., Ahlberg, P. E., Isasi, M. P.,  
876 Arriagada, A., & Chafrat, P. (2012). A new large pterosaur from the Late Cretaceous of  
877 Patagonia. *Journal of Vertebrate Paleontology*, 32(6), 1447–1452.  
878 <https://doi.org/10.1080/02724634.2012.703979>

879 Novas, F. E., Pol, D., Canale, J. I., Porfiri, J. D., & Calvo, J. O. (2009). A bizarre Cretaceous  
880 theropod dinosaur from Patagonia and the evolution of Gondwanan dromaeosaurids.  
881 *Proceedings of the Royal Society B: Biological Sciences*, 276, 1101–1107.  
882 <https://doi.org/10.1098/rspb.2008.1554>

883 O’Gorman, J. P. (2011). Plesiosaurios de la Formación Allen (Campaniano–Maastrichtiano)  
884 en el área del Salitral de Santa Rosa (Provincia de Río Negro, Argentina). *Ameghiniana*, 48,  
885 129–135.

886 Ottone, E. G. (2007). A new palm trunk from the Upper Cretaceous of Argentina.  
887 *Ameghiniana*, 44, 719–725.

888 Passalia, M. G., Garrido, A., Iglesias, A., & Vera, E. I. (2023). The Valcheta Petrified Forest  
889 (Upper Cretaceous), northern Patagonia, Argentina: A geological and paleobotanical survey.  
890 *Cretaceous Research*, 142, 105395.

891 Pérez Pincheira, E., & Garrido, A. C. (2024). Palynostratigraphy from the Allen and Jagüel  
892 formations at the Cerro Gutiérrez locality, Lago Pellegrini area, South Argentina. *Journal of*  
893 *South American Earth Sciences*, 148, 105139. <https://doi.org/10.1016/j.jsames.2024.105139>

894 Reichgelt, T., West, C. K., & Greenwood, D. R. (2018). The relation between global palm  
895 distribution and climate. *Scientific Reports*, 8(1), 4721. [https://doi.org/10.1038/s41598-018-](https://doi.org/10.1038/s41598-018-23147-2)  
896 [23147-2](https://doi.org/10.1038/s41598-018-23147-2)

897 Rigueti, F., Pereda-Suberbiola, X., Ponce, D., Salgado, L., Apesteguía, S., Rozadilla, S., &  
898 Arbour, V. (2022). A new small-bodied ankylosaurian dinosaur from the Upper Cretaceous  
899 of North Patagonia (Río Negro Province, Argentina). *Journal of Systematic Palaeontology*,  
900 20, 2137441. <https://doi.org/10.1080/14772019.2022.2137441>

901 Romero, J. E. (1968). *Palmoxyton patagonicum* n. sp. del Terciario inferior de la provincia de  
902 Chubut, Argentina. *Ameghiniana*, 5, 417–432.

903 Rougier, G. W., Chornogubsky, L., Casadio, S., Arango, N. P., & Giallombardo, A. (2009).  
904 Mammals from the Allen Formation, Late Cretaceous, Argentina. *Cretaceous Research*, 30,  
905 223–238. <https://doi.org/10.1016/j.cretres.2008.07.006>

906 Rozadilla, S., Brissón-Egli, F., Agnolín, F. L., Aranciaga-Rolando, A. M., & Novas, F. E.  
907 (2021). A new hadrosaurid (Dinosauria: Ornithischia) from the Late Cretaceous of northern

908 Patagonia and the radiation of South American hadrosaurids. *Journal of Systematic*  
909 *Palaeontology*, 19, 1207–1235. <https://doi.org/10.1080/14772019.2020.2020917>

910 Salgado, L., & Coria, R. A. (1993). El género *Aeolosaurus* (Sauropoda, Titanosauridae) en la  
911 Formación Allen (Campaniano–Maastrichtiano) de la provincia de Río Negro, Argentina.  
912 *Ameghiniana*, 30, 119–128.

913 Salgado, L., Coria, R. A., Magalhaes Ribeiro, C. M., Garrido, A., Rogers, R., Simón, M. E.,  
914 Arcucci, A. B., Rogers, K. C., Carabajal, A. P., Apesteguía, S., Fernández, M., García, R. A.,  
915 & Talevi, M. (2007). Upper Cretaceous dinosaur nesting sites of Río Negro (Salitral Ojo de  
916 Agua and Salinas de Trapalcó-Salitral de Santa Rosa), northern Patagonia, Argentina.  
917 *Cretaceous Research*, 28, 392–404. <https://doi.org/10.1016/j.cretres.2006.06.007>

918 Sterli, J., de la Fuente, M. S., & Cerda, I. A. (2013). A new species of meiolaniform turtle  
919 and a revision of the Late Cretaceous meiolaniformes of South America. *Ameghiniana*, 50,  
920 240–256.

921 Stenzel, K. G. (1904). Fossile Palmenhölzer. *Beiträge zur Paläontologie und Geologie*  
922 *Österreich–Ungarns und des Orients*, 16, 107–228.

923 Suazo Lara, F., & Gómez, R. O. (2022). In the shadow of dinosaurs: Late Cretaceous frogs  
924 are distinct components of a widespread tetrapod assemblage across Argentinean and Chilean  
925 Patagonia. *Cretaceous Research*, 131, 105085. <https://doi.org/10.1016/j.cretres.2021.105085>

926 Thomas, R. (2011a). *Palm-ID, a database to identify the palm stem anatomy with an expert*  
927 *system (Xper2)*. Université Paris 6 – Muséum national d’Histoire naturelle, Paris. Disponible  
928 en: <http://www.infosyslab.fr/Palm-ID/> (Accessed on September 30th, 2025).

929 Thomas, R. (2011b). *Anatomie comparée des palmiers - Identification assistée par*  
930 *ordinateur, applications en paléobotanique et en archéobotanique* (PhD Thesis, Muséum  
931 National d'Histoire Naturelle, Paris, France). Available from [https://theses.hal.science/tel-](https://theses.hal.science/tel-00951106v1)  
932 [00951106v1](https://theses.hal.science/tel-00951106v1)

933 Thomas, R., & Boura, A. (2015). Palm stem anatomy: phylogenetic or climatic signal?  
934 *Botanical Journal of the Linnean Society*, 178, 467–488. <https://doi.org/10.1111/boj.12274>

935 Thomas, R., & De Franceschi, D. (2012). First evidence of fossil Cryosophileae (Arecaceae)  
936 outside the Americas (early Oligocene and late Miocene of France): Anatomy,  
937 palaeobiogeography and evolutionary implications. *Review of Palaeobotany and Palynology*,  
938 171, 27–39. <https://doi.org/10.1016/j.revpalbo.2011.11.010>

939 Thomas, R., & De Franceschi, D. (2013). Palm stem anatomy and computer-aided  
940 identification: The Coryphoideae (Arecaceae). *American Journal of Botany*, 100, 289–313.  
941 <https://doi.org/10.3732/ajb.1200242>

942 Torres, T., & Godoy, E. (1982). Hallazgo de Palmoxylon chilensis n. sp., del Cretácico  
943 Superior en Huechún, Región Metropolitana. En *Proceedings of the 3rd Congreso Geológico*  
944 *Chileno* (Vol. 1, pp. A302–A320). Concepción, Chile.

945 Vallati, P. (2010). Asociaciones palinológicas con angiospermas en el Cretácico superior de  
946 la Cuenca Neuquina, Argentina. *Revista Brasileira de Paleontologia*, 13, 143–158.  
947 <https://doi.org/10.4072/rbp.2010.2.07>

948 Vera, E. I., Perez Loinaze, V. S., Llorens, M., & Passalia, M. G. (2024). *Palmoxylon*  
949 (Magnoliopsida: Arecaceae) richness in the Puntudo Chico Formation (Campanian-  
950 lowermost Maastrichtian), Chubut Province, Argentina: systematics, palaeoclimatic

951 significance and comments on biogeography of Phytelpeae. *Historical Biology*, 1–16.

952 <https://doi.org/10.1080/08912963.2024.2412151>

953 Von Mohl, H. (1823–1850). De palmarum structura. En K. F. von Martius (Ed.), *Historia*  
954 *naturalis palmarum, Opus tripartitum* (Vol. 1). F. Fleischer.

955

## 956 **Figure legends**

957 **Figure 1.** *Palmoxylon santarosense* Ancibor *emend.* Vera. A, TS of the holotype (BA Pb  
958 887); B, transverse section of the epitype (BA Pb 862); C, detail of B, showing distribution of  
959 fvbs from the center of CZ, through the SZ towards the CT (BA Pb 862); D, distribution of  
960 fvbs in the center of the CZ (BA Pb 862); E, detail of D, showing aspect of fvbs. Notice two  
961 large metaxylem vessels (white arrows), and developed vcap (black arrow) (BA Pb 862). A,  
962 B= 1 cm, C= 3 mm, D=1 mm, and E= 500  $\mu$ m.

963 **Figure 2.** *Palmoxylon santarosense* Ancibor *emend.* Vera. A, distribution of fvbs in the outer  
964 region of the CZ (BA Pb 862); B, C, detail of the distribution of fvbs in the outer region of  
965 the CZ. Notice small ventral projection of the dcap (arrow) (BA Pb 887); D, detail of a single  
966 fvb, showing two wide vessels and phloem region (arrow) (BA Pb 887); E, detail of the  
967 vascular zone of a fvb, showing two wide metaxylem vessels (Xi) and preserved phloem cells  
968 (arrow) (BA Pb 887); F, distribution of fvbs in the most external region of the CZ towards the  
969 SZ. Notice elongate dcap in some fvbs (arrows) (BA Pb 862); G, fvbs in the external region  
970 of the SZ towards the CT, showing a single wide vessel per unit (BA Pb 887); H, detail of the  
971 SZ and CT, showing abundant fibrous bundles in the latter (arrows) (BA Pb 862); I, detail of  
972 the ground tissue in the central region of the CZ, showing isodiametric and elongate  
973 parenchyma cells (BA Pb 862); J, detail of the ground tissue in the external region of the CZ,

974 showing isodiametric parenchyma cells. Notice an ill-preserved fibrous bundle (arrow) (BA  
975 Pb 887); K, Detail of the external region of the SZ and the CT, showing small (black arrows)  
976 and large (white arrow) fibrous bundles (BA Pb 862); L, leaf trace (lt) and vascular bridge  
977 (arrow) (BA Pb 887); M, detail of L, showing a detail of a leaf trace (BA Pb 887); N, detail  
978 of L, showing a vascular bridge (BA Pb 887); O, LS showing vessels and perforation plates  
979 (BA Pb 887); P, LS showing stegmata with globose phytoliths (arrow) (BA Pb 887). Scale  
980 bars: A=1000  $\mu\text{m}$ ; B, F, G, H=500  $\mu\text{m}$ ; C, I=300  $\mu\text{m}$ ; D, K, L, M, O=200  $\mu\text{m}$ ; E, J, N, P=100  
981  $\mu\text{m}$ .

982 **Figure 3.** *Palmoxylon santarosense* Ancibor *emend.* Vera. A, two TS of the specimen BA Pb  
983 944. Notice the presence of the holotype of *Stipitichnus koppae* Genise, 1995 (MACN-Icn  
984 123), traces interpreted as insect borings, in the upper image (arrows). B, detail of A, showing  
985 distribution of fvbs in the outer preserved region of the stem; C, detail of B, showing fvbs; D,  
986 detail of A, showing distribution of fvbs in the center of the stem. E, detail of D, showing  
987 fvbs. Scale bars: A=2 cm; B, D = 2 mm; C, E=1 mm.

988 **Figure 4.** *Palmoxylon rionegrense* Ancibor *emend.* Vera. A, TS of the holotype (BA Pb 884);  
989 B, distribution of fvbs towards the center of the stem (BA Pb 884); C, detail of A, showing  
990 distribution of fvbs in the fossil (preserving only the CZ), from the center of the stem (CZin)  
991 towards the exterior (CZout) (BA Pb 884); D, fvbs in the center of the stem (BA Pb 884); E,  
992 fvbs in the outermost preserved region of the stem (BA Pb 884); F, detail of a fvb showing  
993 two large vessels (BA Pb 884); G, detail of a fvb showing three large vessels (BA Pb 884); H,  
994 detail of the vascular region of a fvb with two large vessels. Notice fibers of the vcap (white  
995 arrow) and dcap (black arrow) (Ba Pb 884); I, detail of the vascular region of a fvb with four  
996 large vessels (arrows) (Ba Pb 884); J, detail of the vascular region of a fvb with three large  
997 vessels (Ba Pb 884); K, ground tissue and interspersed fvbs. Notice elongate parenchymatous

998 cells (white arrows) and tabular parenchyma (black arrows) (BA Pb 884). Scale bars: A= 2  
999 cm; B=2 mm; C=3 mm; D, E= 500  $\mu\text{m}$ ; F, G, H, K= 200  $\mu\text{m}$ ; I, J=100  $\mu\text{m}$ .

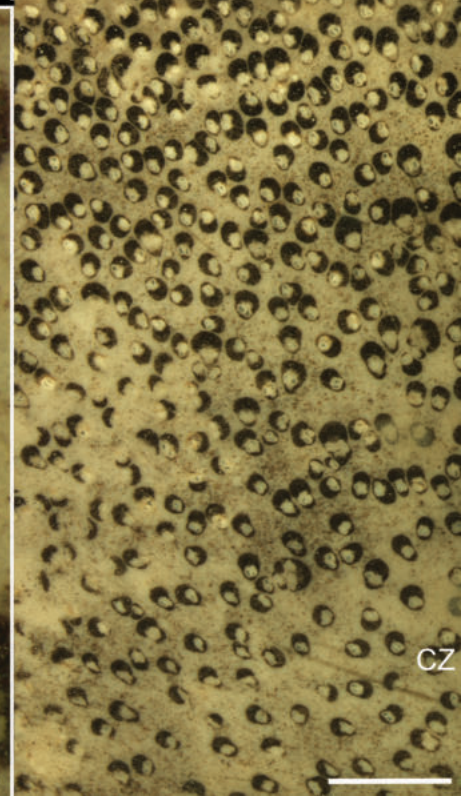
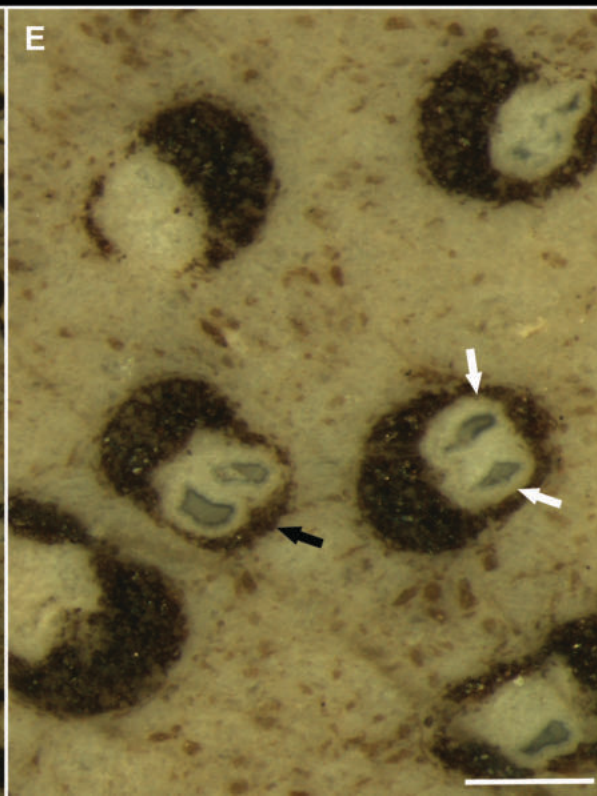
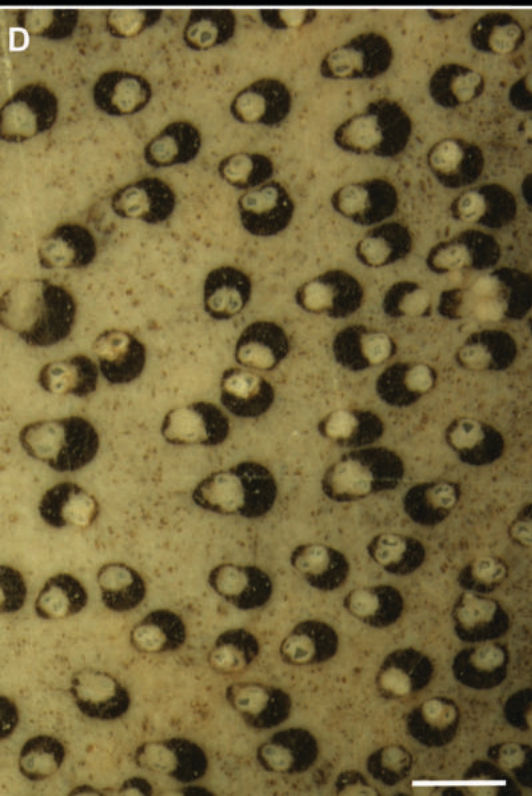
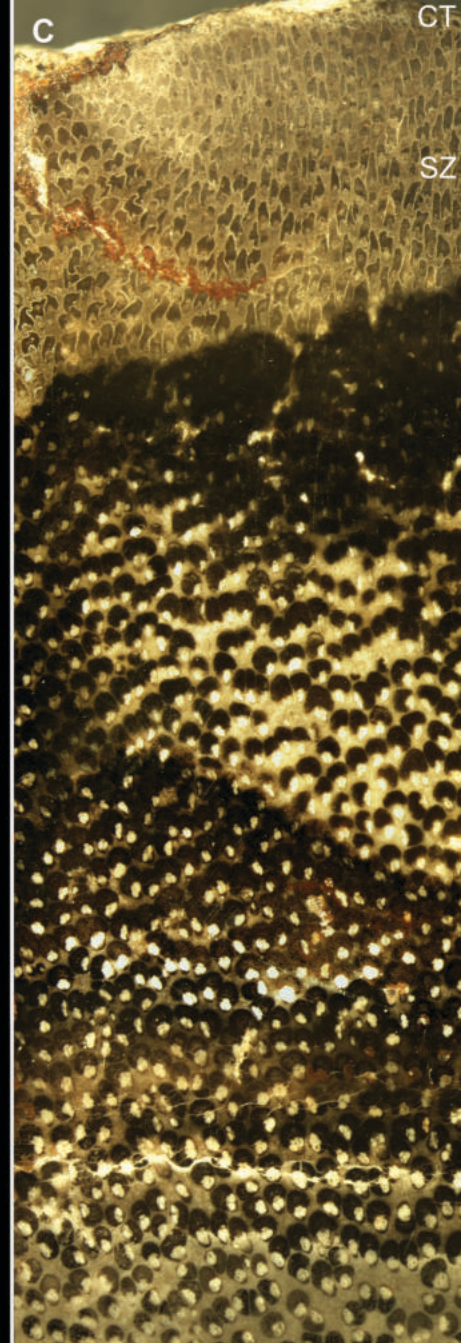
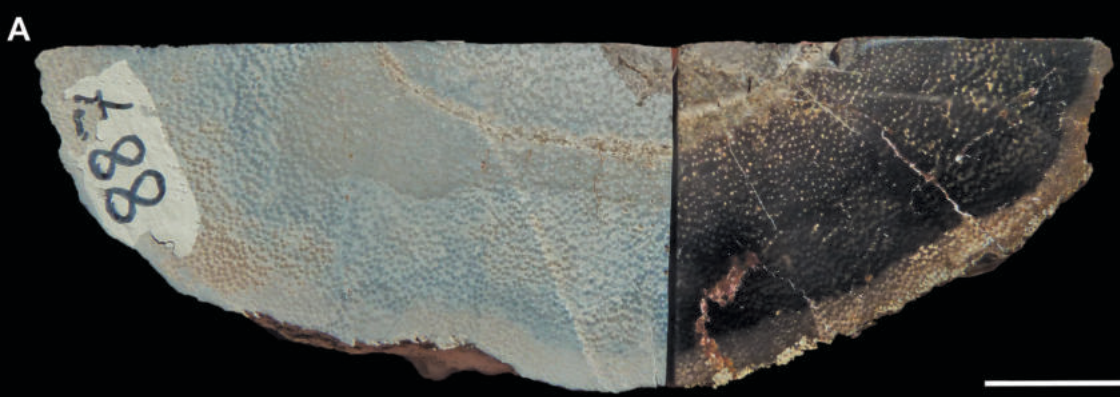
1000 **Figure 5.** *Palmoxylon rionegrense* Ancibor emend. Vera. A, B, TS showing a leaf trace with  
1001 two vascular units (white arrows). Notice vascular bridge in A (black arrow) (BA Pb 884); C,  
1002 detail of the two-parted vascular zone of the leaf trace (white arrows) (BA Pb 884); D, detail  
1003 of a vascular bridge (BA Pb 884); E, LS showing stegmata with globose phytoliths (white  
1004 arrows) and lacunae in ground tissue (black arrows) (BA Pb 884); F, G, LS showing stegmata  
1005 with conical phytoliths (arrows) (BA Pb 884). Scale bars: A, B=300  $\mu\text{m}$ ; C, D, E, F, G =100  
1006  $\mu\text{m}$ .

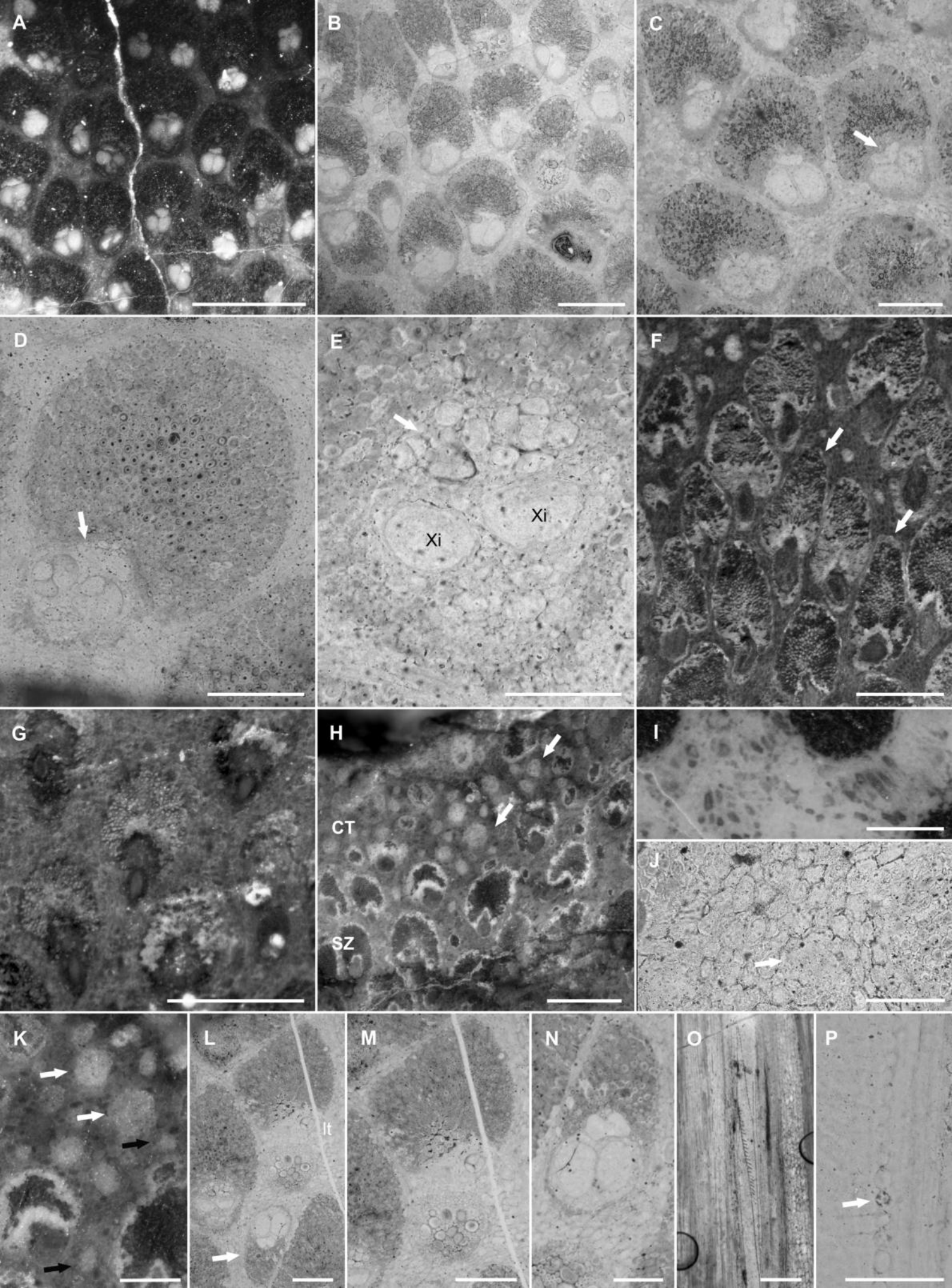
1007 **Figure 6.** *Palmoxylon valchetense* Ancibor emend. Vera. A, transverse (top) and longitudinal  
1008 (bottom) view of the holotype (BA Pb 890); B, transverse section of specimen BA Pb 888; C,  
1009 transverse section of specimen BA Pb 889, previously included in *P. rionegrense*; D,  
1010 transverse view of the epitype (BA Pb 967); E, detail of D, showing distribution of fvb from  
1011 the CZ to the CT (BA Pb 967); F, detail of a fvb of the CZ in the holotype (BA Pb 890); G,  
1012 detail of a fvb of the center CZ (BA Pb 888); H, detail of a fvb of the CZ in the epitype (BA  
1013 Pb 967); I, detail of a fvb in the outer region of the CZ/SZ in the epitype (BA Pb 967); J,  
1014 detail of a fvb in the outer region of the CZ/SZ in the specimen previously included in *P.*  
1015 *rionegrense* (BA Pb 889); K, detail of a fvb with elongated dcap in the SZ of the epitype (BA  
1016 Pb 967); L, detail of the fibres of the dcap (white arrow) and tabular parenchyma (black  
1017 arrow) (BA Pb 890). Scale bars: A, B= 1 cm; C, E=2 cm; F, G, H, I, J, K=500  $\mu\text{m}$ ; L=100  
1018  $\mu\text{m}$ .

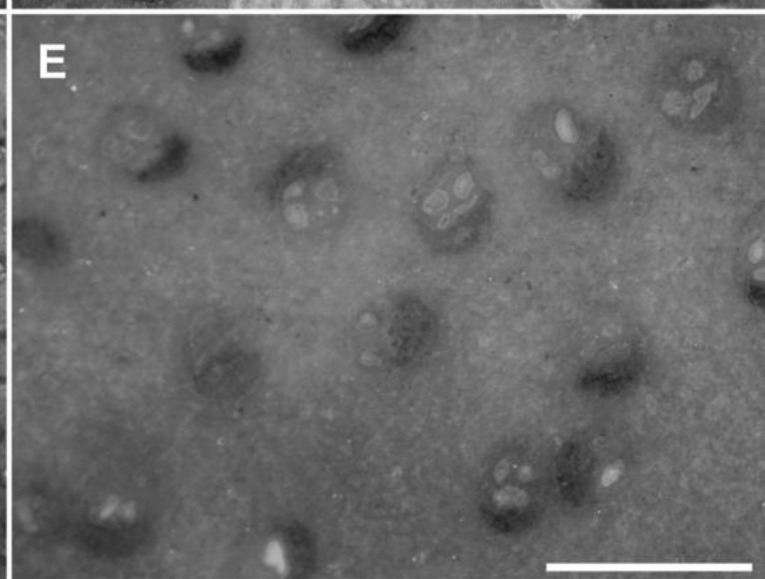
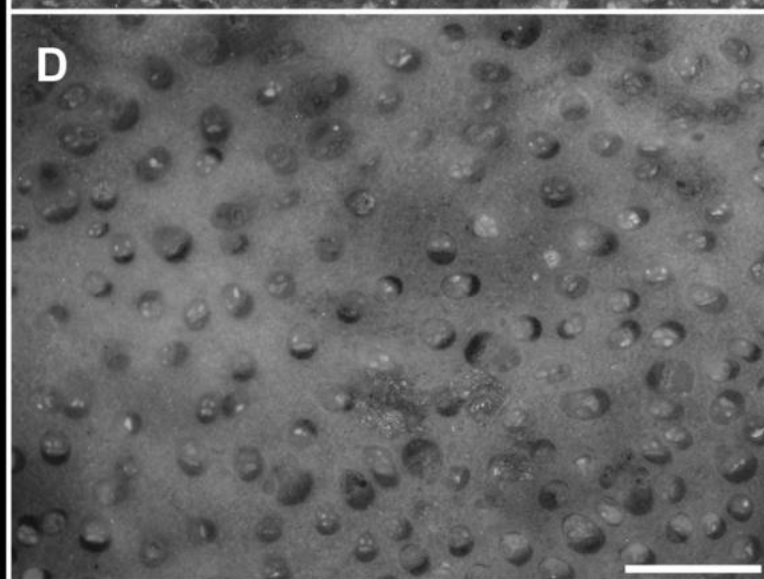
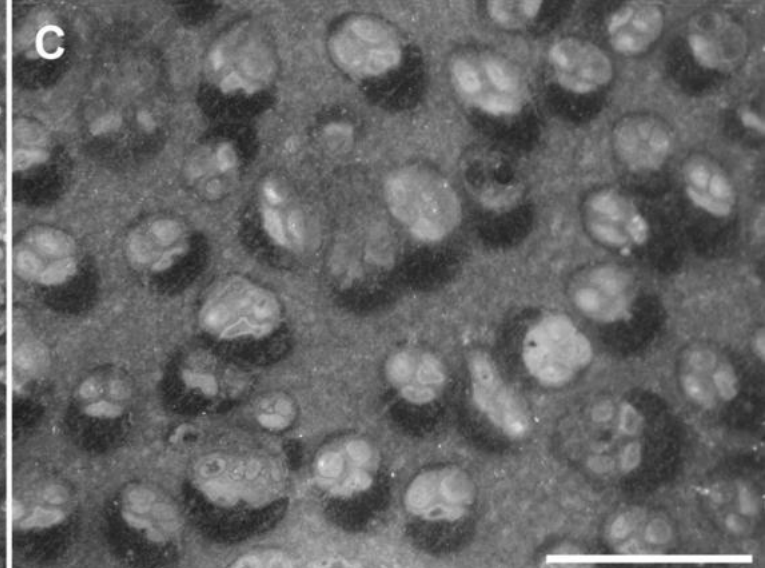
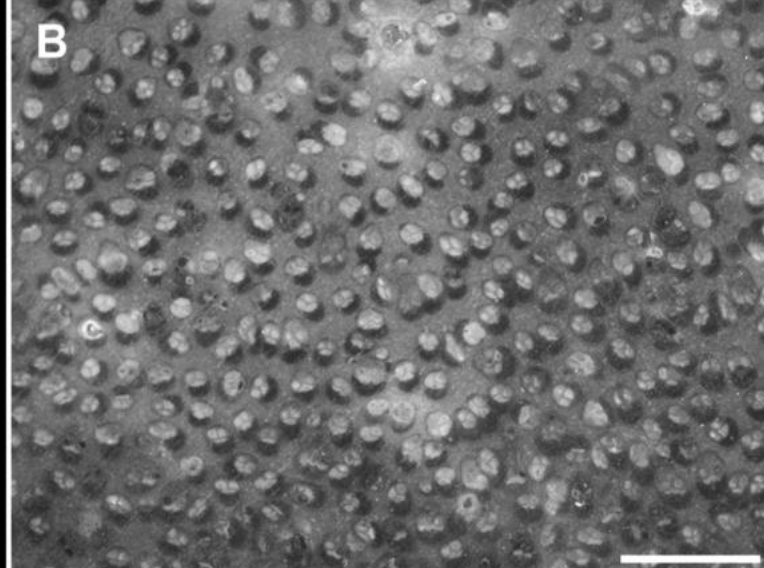
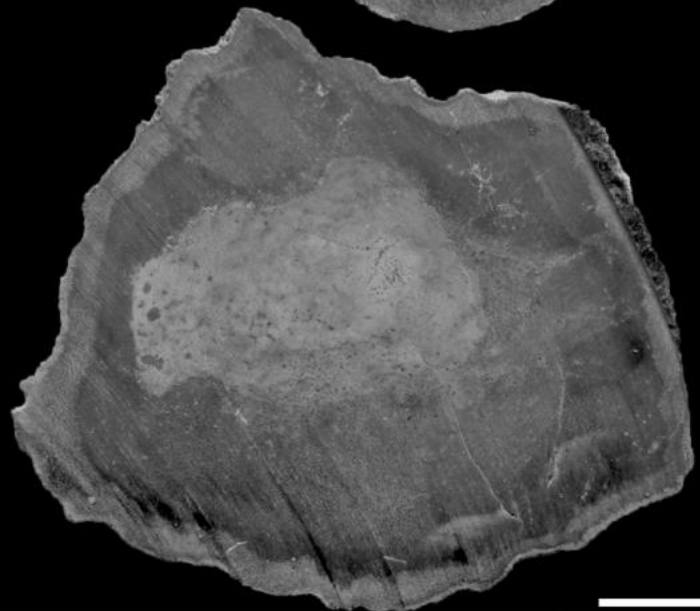
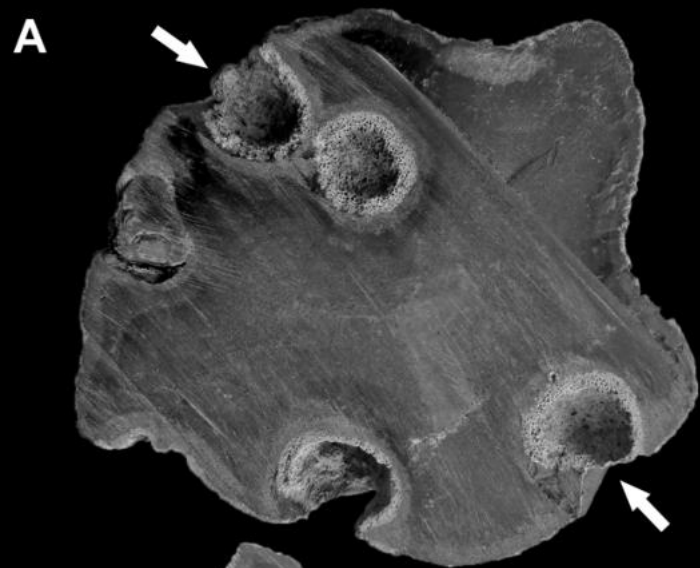
1019 **Figure 7.** *Palmoxylon valchetense* Ancibor emend. Vera. A, detail of the vascular zone of a  
1020 fvb, showing two wide metaxylem vessels and developed paravascular parenchyma. Notice  
1021 the ventral projection of the dcap into the phloem strand (arrow) (BA Pb 890); B, detail of the

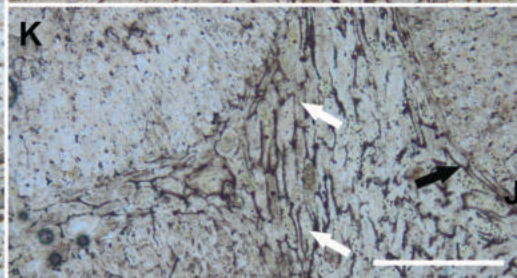
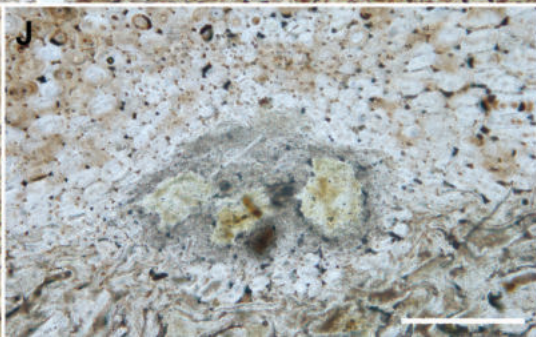
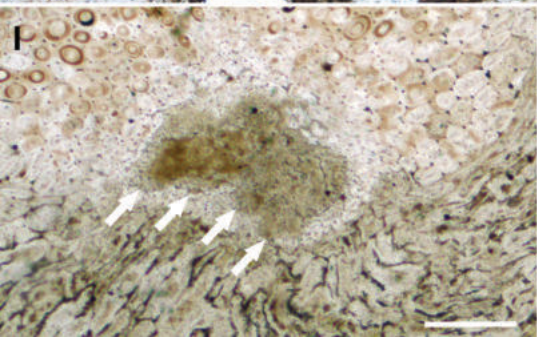
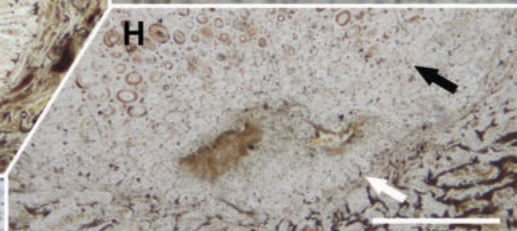
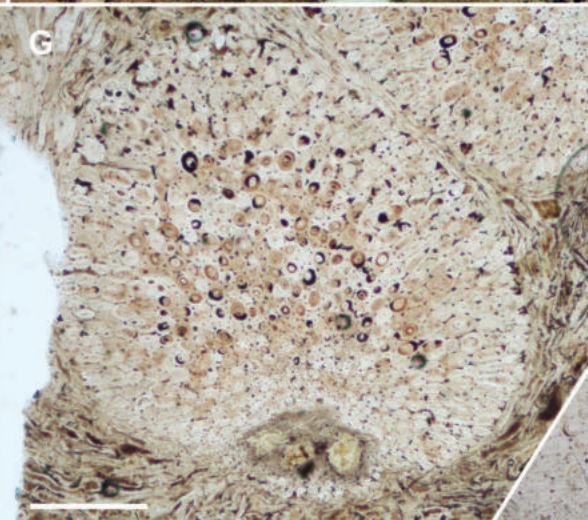
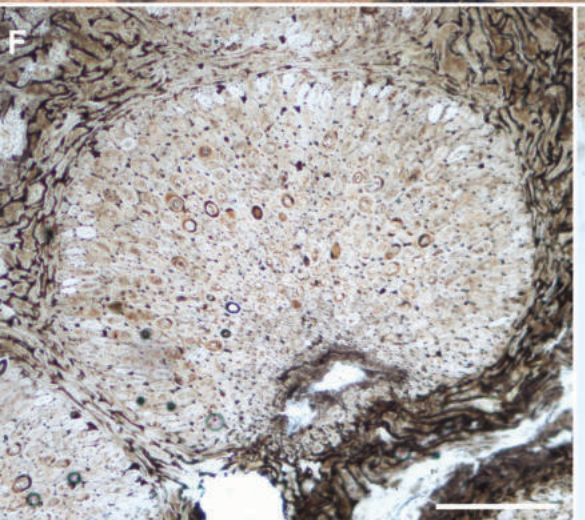
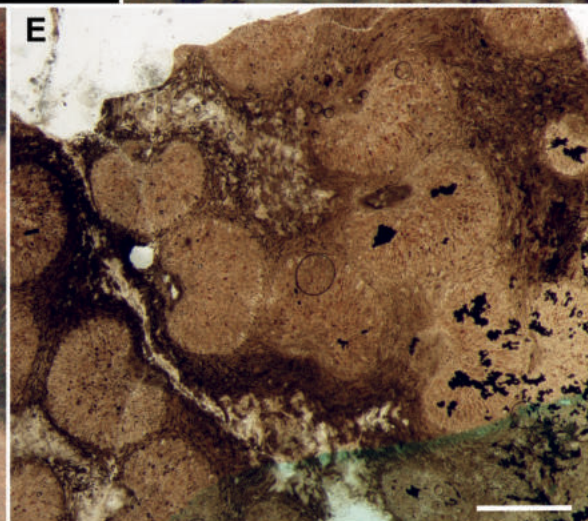
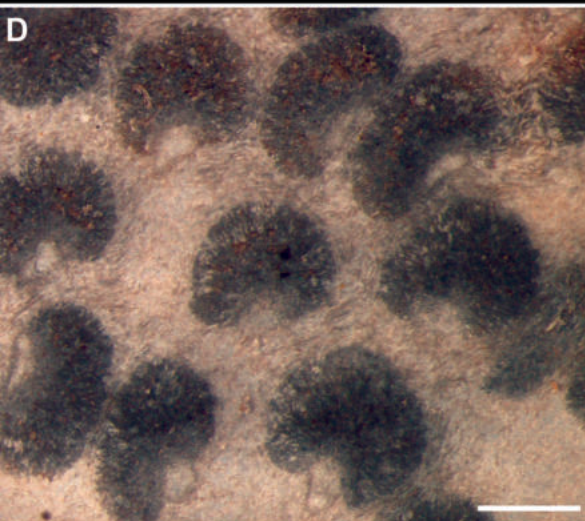
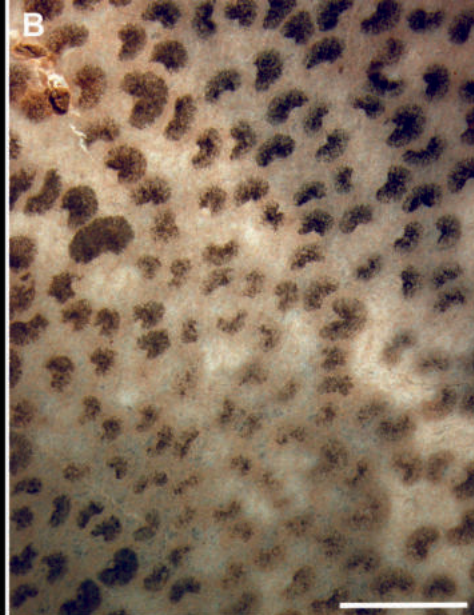
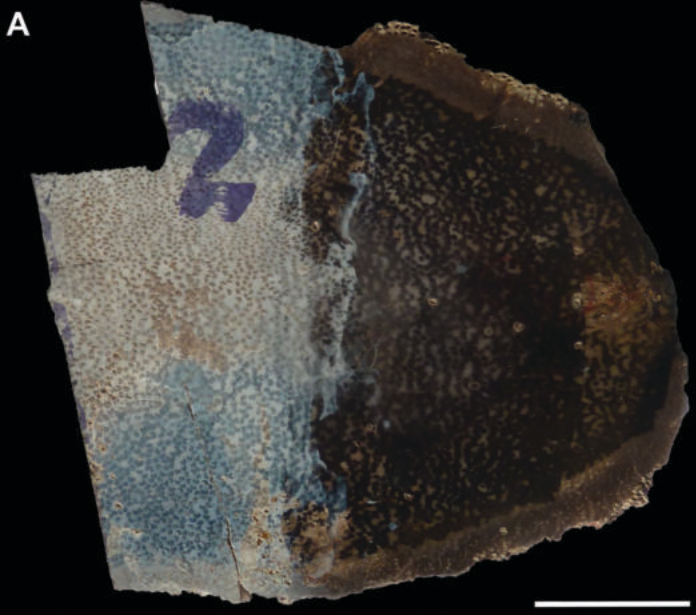
1022 vascular zone of a fvb, showing four wide metaxylem vessels (BA Pb 890); C, detail of the  
1023 vascular zone of a fvb, showing two wide metaxylem vessels and developed paravascular  
1024 parenchyma (black arrow). Notice the ventral projection of the dcap into the phloem strand  
1025 (white arrow) (BA Pb 888). D, detail of a fvb, showing polygonal xylem elements between  
1026 the two large wide vessels (white arrows), and radially elongate fibers of the vcap (black  
1027 arrows) (BA Pb 890); E, aspect and distribution of fvbs in the CZ (BA Pb 967); F, aspect and  
1028 distribution of fvbs in the TZ (BA Pb 967); G, aspect of the SZ. Notice the presence of  
1029 fibrous bundles (arrows) (BA Pb 967); H, detail of the outer region of the SZ and the  
1030 preserved portion of the CT, showing abundant fibrous bundles (arrows) (BA Pb 967); I,  
1031 detail of the ground tissue, showing parenchymatous cells with thickened walls (white  
1032 arrows). Notice the vcap of a fvb, with elongated cells (black arrow) (BA Pb 890); J, detail of  
1033 the ground tissue in the SZ, showing fibrous bundles (arrows) (BA Pb 889); K, detail of J,  
1034 showing a fibrous bundle (BA Pb 889); L, comparison between fvbs and a leaf trace (black  
1035 arrow). Notice the small vascular bridge (white arrow) (BA Pb 890); M, detail of a leaf trace  
1036 (BA Pb 890); N, detail of a vascular bridge (BA Pb 890); O, longitudinal section showing  
1037 stigmata with globose phytoliths (BA Pb 890). Scale bars: A, B, C, J, N=200  $\mu$ m; D, I, K=  
1038 100  $\mu$ m; E, F, G, H, L= 1 mm; M=500  $\mu$ m; O=50  $\mu$ m

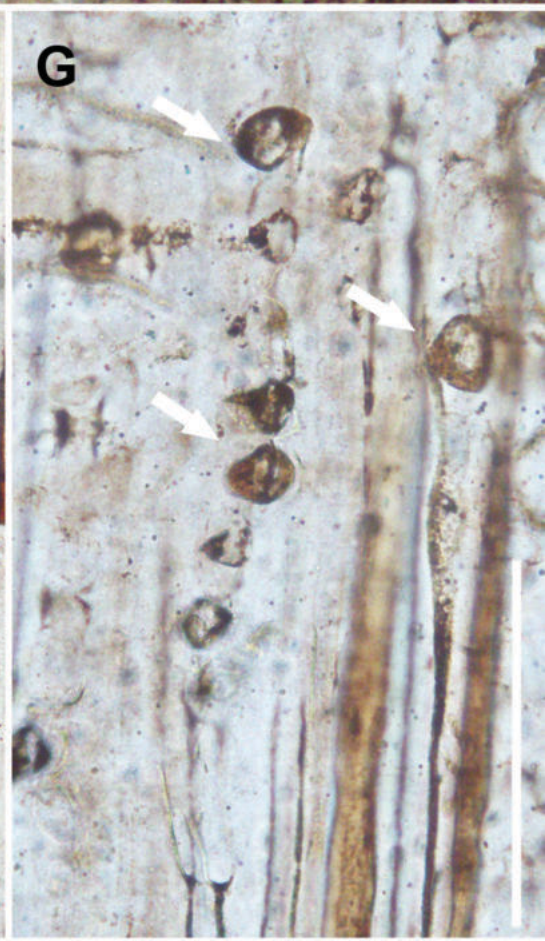
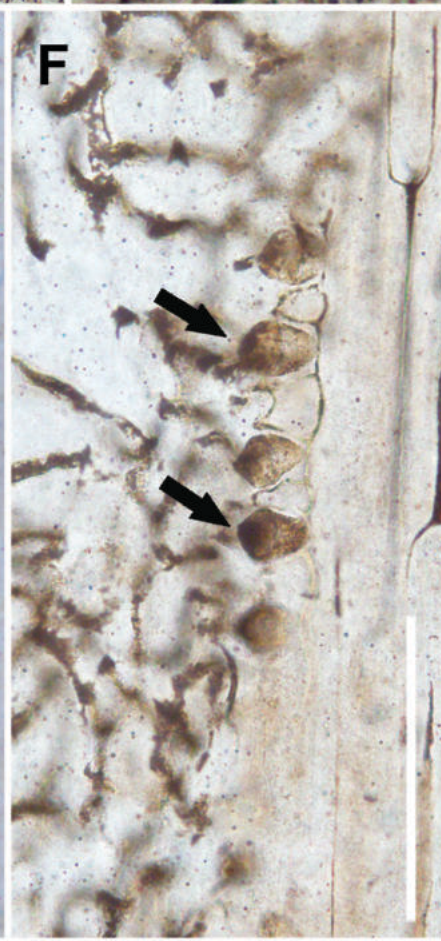
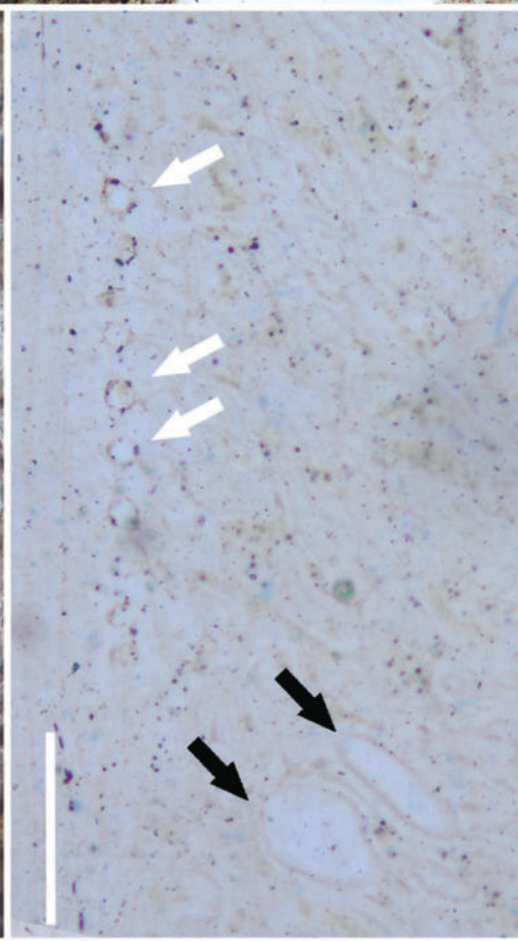
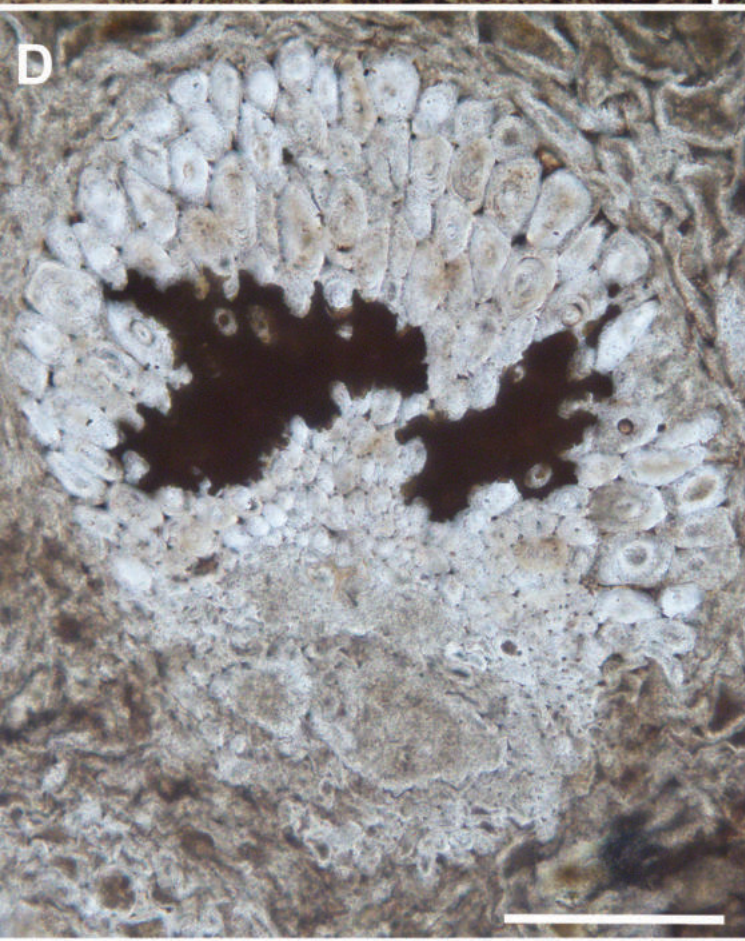
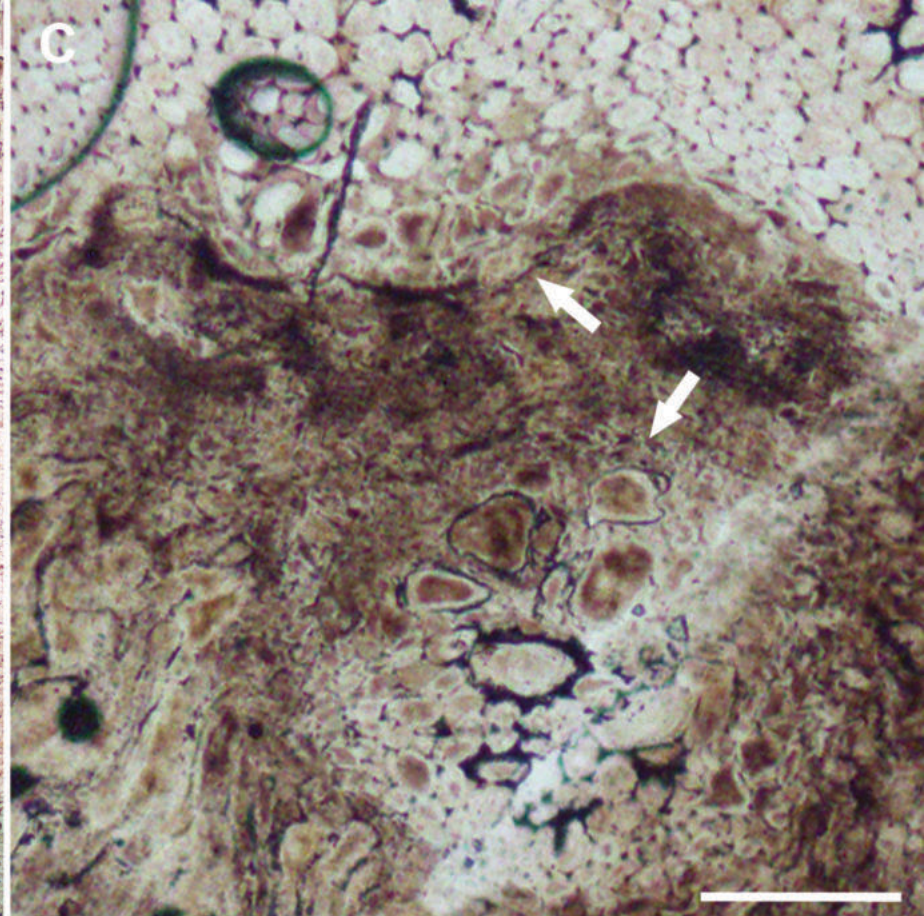
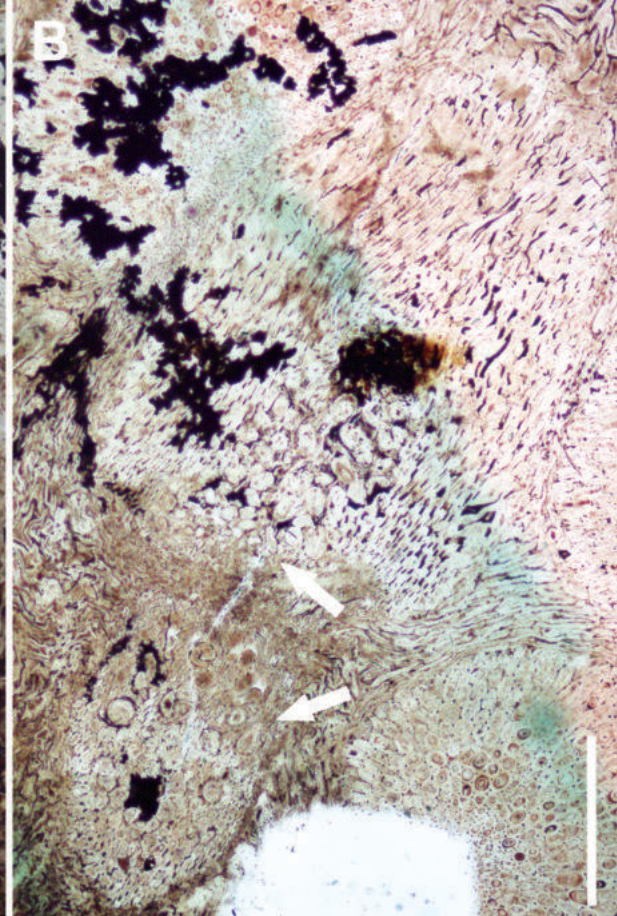
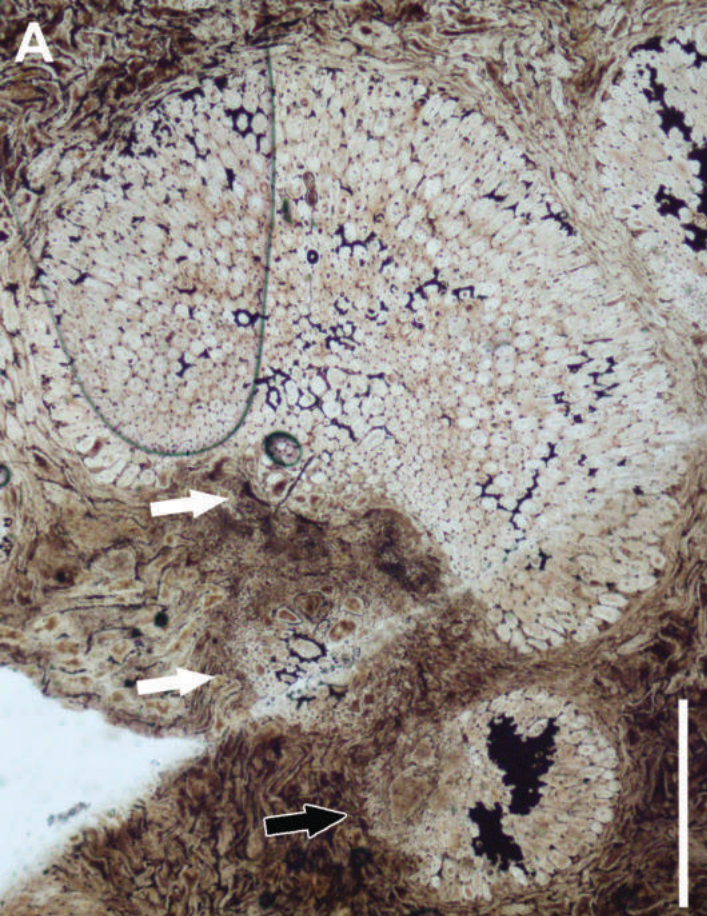
1039 **Table 1.** Comparison between *Palmoxylon* remains of the Allen Formation and other South  
1040 American taxa. Abbreviations: dcap shape: morphology of the fibrous region adjacent to the  
1041 phloem in the fibrovascular bundle (*sensu* Stenzel, 1904); vcap: presence of fibrous sheath  
1042 adjacent to the xylem in the fibrovascular bundles; RP: radial parenchyma; TP: tabular  
1043 parenchyma. Anatomical data taken from Ancibor (1995), Martínez (2012), Martínez *et al.*  
1044 (2023), Torres and Godoy (1982), Ottone (2007); Romero (1968); Arguijo (1979, 1981),  
1045 Franco (2014); Franco *et al.* (2014), Lutz (1980, 1984, 1986), and Vera *et al.* (2024).

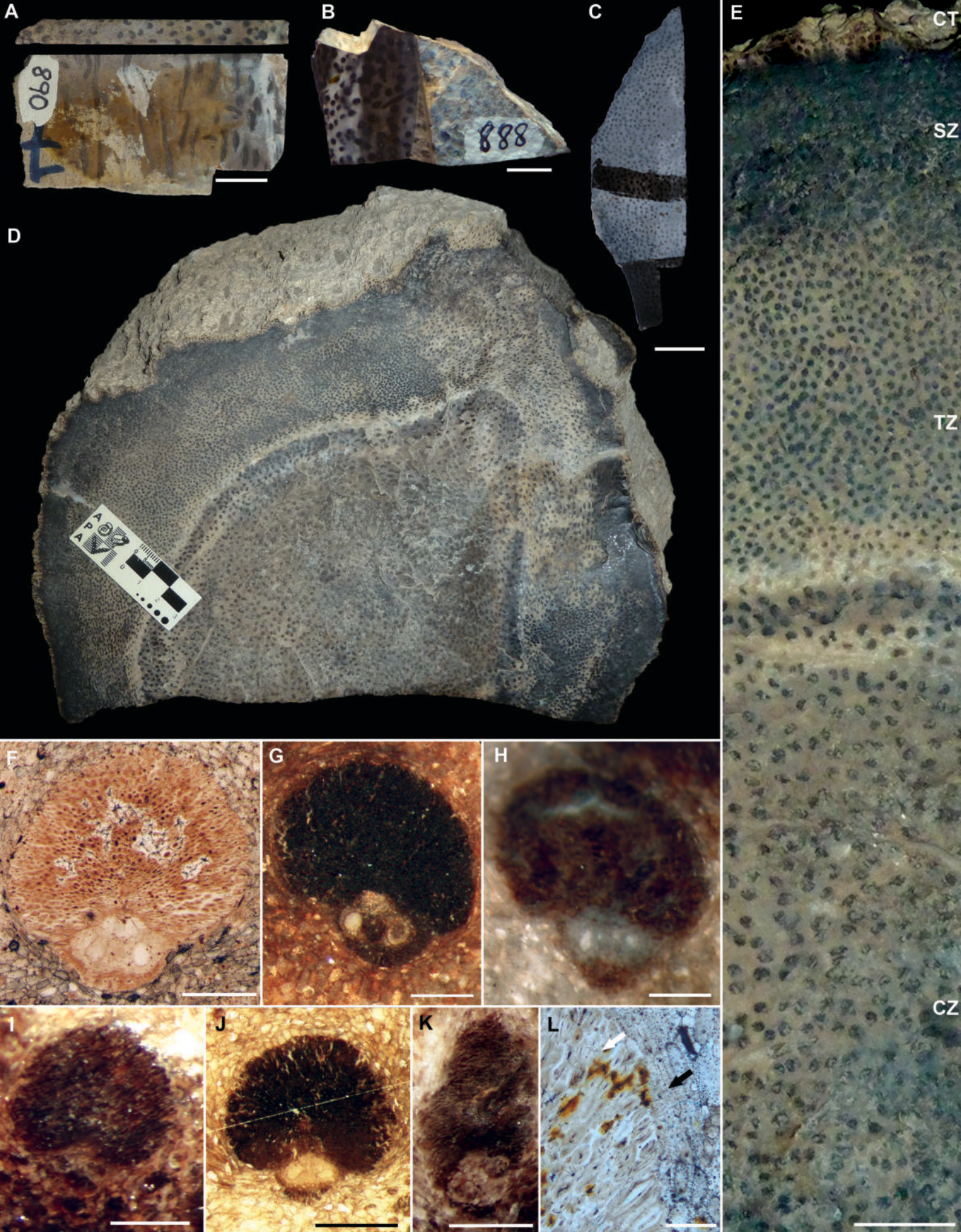


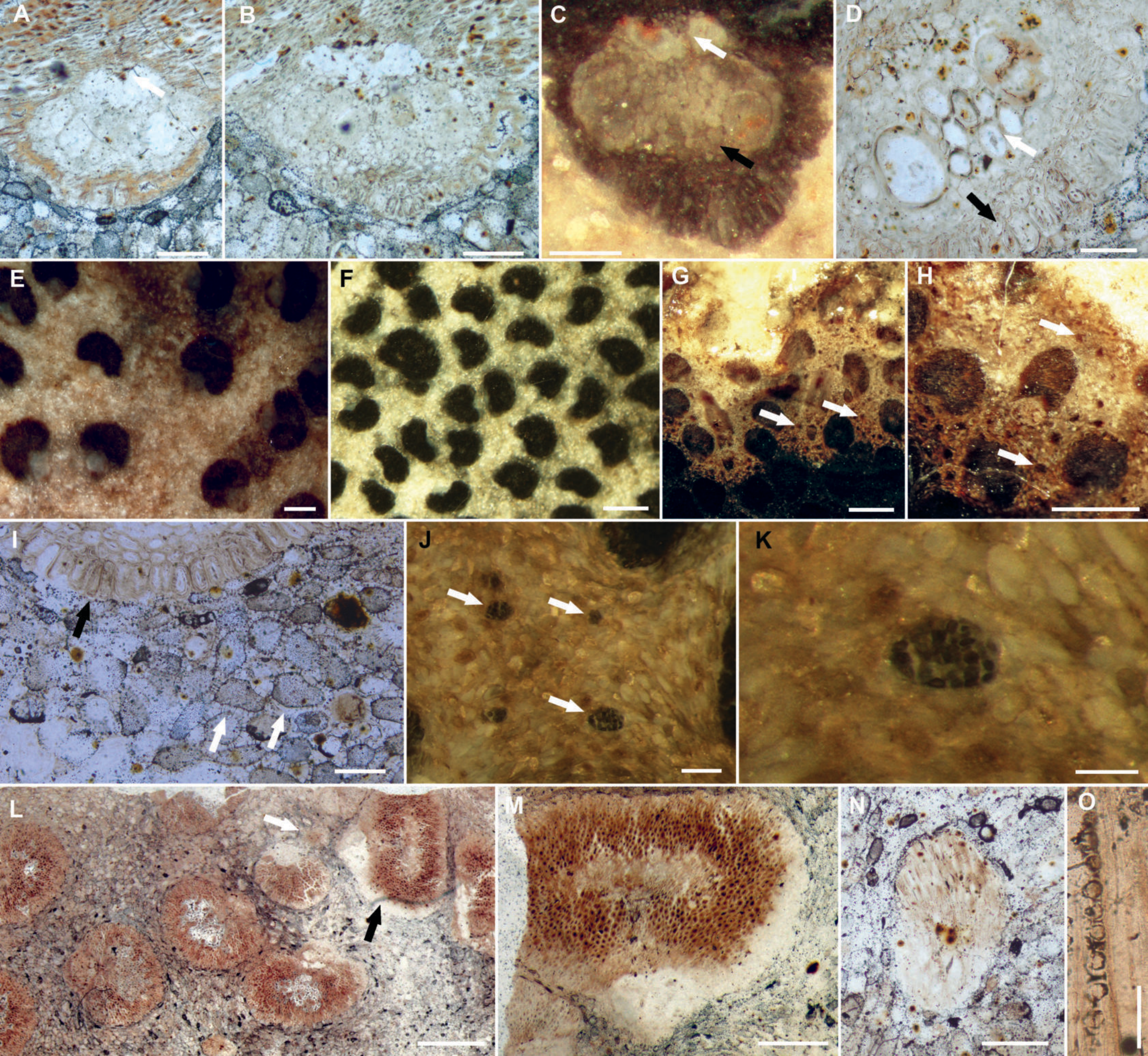












Taxon	Formation and age	Mx	dcap shape	vcap	Ph	RP	TP	ground tissue cells	fb	Phy
<i>P. santarosense</i> Ancíbor emend. Vera	Allen; uCmp - Maa	1 (CZ), 2 (SZ)	Lu-Va (CZin), Re (CZout), Re/Sa (SZ)	yes	1	no	yes	isodiametric, slightly elongate (CZ /SZ) + elongate (CZ)	in CZout, SZ and CT	GLO
<i>P. rionegrense</i> Ancíbor emend. Vera	Allen; uCmp - Maa	2(2–4)	Re	yes	?	no	yes	highly elongate, with scarce lacunae	No	GLO & CON
<i>P. valchetense</i> Ancíbor emend. Vera	Allen; uCmp - Maa	2(1–4)	Re	yes	1–2	no	yes	isodiametric, elongate	Scarce (CZ), abundant (SC, CT)	GLO
<i>P. garridoi</i> Martínez 2012	Anacleto; Cmp	3 (2–6)	Re/Va	no	1	no	yes	elongate, rhombohedral, sometimes rod- like, constituting an irregular network, delimiting lacunae	No	GLO
<i>P. sp. 1</i> in Vera <i>et</i> <i>al.</i> (2024)	Puntudo Chico; Cmp - Ist Maa	2(3–4)	Re	no	1	no	?	isodiametric, elongate, rhombohedral, sometimes rod-like	Yes	?
<i>P. sp. 2</i> in Vera <i>et</i> <i>al.</i> (2024)	Puntudo Chico; Cmp - Ist Maa	2(3–4)	Lu/Va	yes	1	no	yes	isodiametric, with elongate cell strands	Yes	?
<i>P. sp. 3</i> in Vera <i>et</i> <i>al.</i> (2024)	Puntudo Chico; Cmp - Ist Maa	1	Re	yes	1	no	?	elongate, rhombohedral, sometimes rod- like, constituting an irregular network, delimiting lacunae	No	?
<i>P. sp. 4</i> in Vera <i>et</i> <i>al.</i> (2024)	Puntudo Chico; Cmp - Ist Maa	1(2)	Re	no	?	no	yes	isodiametric, with elongate cell strands	yes	?
<i>P. sp. cf. P.</i> <i>phytelephantoides</i> Chate <i>et al.</i> 2019 in Vera <i>et al.</i> (2024)	Puntudo Chico; Cmp - Ist Maa	more than 10, angular	Co	no	1	no	yes	isodiametric	yes	?
<i>P. subantarcticae</i> Martínez <i>et</i> Leppe, 2023	Dorotea; Maa	3(1–6)	Re	yes	1	no	yes	elongate, rhombohedral, sometimes rod- like, constituting an irregular network, delimiting lacunae	yes	GLO
<i>P. chilensis</i> Torres <i>et</i> Godoy 1982	?; uK? - Pg?	1	Cm	yes	1	yes	yes	isodiametric without lacunae, to lacunate	In CT	?

<i>P. pichaihuensis</i> Ottone 2007	Pichaihue Limestone; Dan	1–5	Re	no	?	?	?	unclear, irregular	no	?
<i>P. patagonicum</i> Romero 1968	Salamanca ; Dan	2(1–4)	Cm/Co	no	1–2	yes	yes	isodiametric to slightly elongate, rarely showing lacunae	yes	GLO & CON
<i>P. bororoense</i> Arguijo 1979	Cerro Bororó; Dan	2–4	Va/Lu	yes	?	no	yes	isodiametric	yes	GLO
<i>P. vaterum</i> Arguijo 1981	Cerro Bororó; Dan	2(3–7)	Va	yes	1–2	yes	yes	isodiametric	yes	GLO
<i>P. romeroi</i> Franco <i>et al.</i> 2014	Chiquimil; Mio	3–4(3–5)	Va	yes	1	yes	yes	isodiametric, elongate, undulating	no	GLO
<i>P. concordiense</i> Lutz 1980 emend. Lutz 1986	Salto Chico; Pli	2	Sa/Cm/Co	no	1	yes	yes	isodiametric, elongate	yes	GLO
<i>P. yuqueriense</i> Lutz 1984	Salto Chico / Ituzaingó; Pli	2	Cm/Co/Lu	no	1	yes	yes	isodiametric	no	GLO

Table 1. Comparison between *Palmoxylon* remains of the Allen Formation and other South American taxa. Abbreviations: Mx: number of wide metaxylem elements in fvbs; Ph: number of phloem strands in fvbs; RP: radiating parenchyma; TP: tabular parenchyma; fb: fibrous bundles in ground tissue; Phy: phytoliths; Cmp: Campanian; Maa: Maastrichtian; Dan: Danian; K: Cretaceous; Pg: Paleogene; Mio: Miocene; Pli: Pliocene; u: upper/Upper; Ist: lowermost; Lu: Lunaria; Va: Vaginata; Co: Cordata; Re: Reniforma; Cm: Complanata; Sa: Sagittata; CZin: inner region of the CZ; CZout: outer region of the CZ; GLO: globular; CON: conical. Anatomical data taken from Ancibor (1995), Martínez (2012), Martínez et al (2023), Torres and Godoy (1982), Ottone (2007); Romero (1968); Arguijo (1979, 1981), Franco (2014); Franco et al. (2014), Lutz (1980, 1984, 1986), and Vera et al. (2024).